

Slaying Axion-Like Particles via Gravitational Waves and Primordial Black Holes from Supercooled Phase Transition

Angela Conaci,^{a,b} Luigi Delle Rose,^{a,b} P. S. Bhupal Dev,^c Anish Ghoshal^d

^a Dipartimento di Fisica, Università della Calabria,
I-87036 Arcavacata di Rende, Cosenza, Italy

^b INFN-Cosenza, I-87036 Arcavacata di Rende, Cosenza, Italy

^c Department of Physics and McDonnell Center for the Space Sciences,
Washington University, St. Louis, Missouri 63130, USA

^d Institute of Theoretical Physics, Faculty of Physics, University of Warsaw,
ul. Pasteura 5, 02-093 Warsaw, Poland

E-mail: angela.conaci@unical.it, luigi.dellerose@unical.it, bdev@physics.wustl.edu,
anish.ghoshal@fuw.edu.pl

Abstract. We study the formation of primordial black holes (PBHs) from density fluctuations due to supercooled phase transitions (PTs) triggered in an axion-like particle (ALP) model. We find that the mass of the PBHs is inversely correlated with the ALP decay constant f_a . For instance, for f_a varying from $\mathcal{O}(100 \text{ MeV})$ to $\mathcal{O}(10^{12} \text{ GeV})$, the PBH mass varies between $(10^3 - 10^{-24})M_\odot$. We then identify the ALP parameter space where the PBH can account for the entire (or partial) dark matter fraction of the Universe, in a single (multi-component) dark matter scenario, with the ALP being the other dark matter candidate. The PBH parameter space ruled out by current cosmological and microlensing observations can thus be directly mapped onto the ALP parameter space, thus providing new bounds on ALPs, complementary to the laboratory and astrophysical ALP constraints. Similarly, depending on the ALP couplings to other Standard Model particles, the ALP constraints on f_a can be translated into a lower bound on the PBH mass scale. Moreover, the supercooled PT leads to a potentially observable stochastic gravitational wave (GW) signal at future GW observatories, such as aLIGO, LISA and ET, that acts as another complementary probe of the ALPs, as well as of the PBH dark matter. Finally, we show that the recent NANOGrav signal of stochastic GW in the nHz frequency range can be explained in our model with $f_a \simeq (10 \text{ GeV} - 1 \text{ TeV})$.

Contents

1	Introduction	1
2	The supercooled ALP phase transition	4
2.1	Finite-temperature effects	5
2.2	An explicit ALP realization	7
3	GW signals from supercooled ALP phase transition	8
4	PBH formation from supercooled ALP phase transition	10
5	Numerical results	12
5.1	GW-PBH complementarity	12
5.2	The astrophysical foreground	15
5.3	Fitting the NANOGrav signal	16
5.4	PBH constraints	16
6	Complementarity with laboratory and astrophysical ALP searches	19
7	Discussion and Conclusion	21
A	Supplementary plots	22

1 Introduction

The first direct detection of gravitational waves (GWs) by the LIGO-VIRGO collaboration [1] has opened up new avenues to explore the Universe. The known astrophysical sources of GWs can be broadly split into three categories [2]: (i) transient signals (with a duration between a millisecond and several hours) emitted by the merger of two compact objects, like black hole or neutron star binaries, or supernova core collapse; (ii) long-duration (or steady-state) signals, e.g. from spinning neutron stars or from binary white-dwarf mergers; and (iii) stochastic background arising from the superposition of unresolved astrophysical sources. Stochastic GW background (SGWB) is also a unique probe of the early Universe, as the Universe is transparent to GWs right from the wee moments of the Big Bang, unlike other cosmic relics like photons and neutrinos. Although LIGO-VIRGO has only set an upper limit on the SGWB [3–5], the increased sensitivity of future GW detectors in a wide frequency range from nHz-kHz, such as SKA [6], GAIA/THEIA [7], MAGIS [8], AION [9], AEDGE [10], μ ARES [11], LISA [12], TianQin [13], Taiji [14], DECIGO [15], BBO [16], ET [17], CE [18], as well as recent proposals for high-frequency GW searches in the MHz-GHz regime [19–22], makes the future detection of SGWB an exciting real possibility. The recent evidence supporting the existence of a SGWB coming from several Pulsar Timing Arrays (PTAs), namely, NANOGrav [23], EPTA [24], PPTA [25] and CPTA [26], has added fuel to the excitement and opened a floodgate of papers with various interpretations, from mundane astrophysics to exotic new physics; see e.g. Refs. [27–29].

Among various cosmological mechanisms for producing a SGWB [30], cosmological first-order phase transitions (FOPTs) [31] stand out as a unique probe of beyond the Standard

Model (BSM) physics, up to remarkably high scales. This is because the SM predicts only two (electroweak and QCD) phase transitions, none of which can be of first-order [32, 33]. Therefore, the detection of a GW signal compatible with a FOPT would be a clear evidence of BSM physics. FOPTs develop by the formation of bubbles that expand, collide and percolate. The violent collisions between the bubble walls (and the motion of the surrounding thermal plasma) lead to the production of stochastic GWs that permeate the Universe as a relic cosmological background radiation analogous to the cosmic microwave background (CMB) radiation. The temperature T of the plasma at the end of the FOPT is directly captured by the power spectrum of the GW signal observed today, with the frequency at the peak of the signal scaling as $f_{\text{peak}} \propto T$. An FOPT at the electroweak scale of $T \sim 100$ GeV peaks around mHz [34] which is in the frequency sensitivity band of space-based GW experiments such as LISA [12], whereas ground-based experiments such as LIGO-VIRGO [35, 36] and ET [17] with a frequency band in the 100 Hz range, are capable of probing FOPTs up to $T \sim 10^8$ GeV [37], well beyond the reach of any foreseeable collider experiment.

Interestingly, the FOPT energy scale LIGO is sensitive to roughly coincides with the lowest possible energy scale at which the global Peccei-Quinn (PQ) symmetry $U(1)_{\text{PQ}}$ has to be broken in QCD axion models that solve the strong CP problem of the SM [38–41]. Axion can also be a viable cold dark matter (DM) candidate [42–44]. Even more generally, axion-like particles (ALPs) are well-motivated, as they naturally appear as pseudo Nambu-Goldstone bosons in many BSM extensions with a spontaneously broken global $U(1)$ symmetry, e.g. in string theory realizations [45–47], in models of natural inflation [48–50], baryogenesis [51–56] and dark energy [57–62], in the relaxion mechanism for solving the hierarchy problem [63], or in unified ultraviolet-completions of the SM [64–68]. If the $U(1)$ symmetry breaking happens to be of first-order and strong enough, it can potentially lead to an observable SGWB at current or future GW detectors [69–71]. In the past years, this aspect raised limited interest because the low-energy ALP phenomenology relevant for laboratory experiments does not depend on the nature of the PT. Today, however, the situation is rather different, since the opportunity of observing GW signals is concrete and offers a uniquely powerful way to *directly* test the high-scale PQ dynamics, in a way complementary to various laboratory and astrophysical probes of the ALP couplings to the SM particles [72] which go as the inverse of the PQ scale, with model-dependent $\mathcal{O}(1)$ coefficients [73–76]. Moreover, the viable parameter space for ALP masses and couplings spans many orders of magnitude, which makes it challenging to completely rule it out; therefore, new ideas and approaches to probe previously inaccessible regions are worth paying attention to. For instance, if the ALP is effectively decoupled from the SM, the only bound may come from black hole superradiance [77]. The GW signal from a FOPT induced by ALPs is another such probe which only depends on the $U(1)$ breaking scale but not on the ALP mass.

In this context, the most important requirement is that the PT must be of strongly first-order so that a detectable GW signal is produced. This condition is automatically fulfilled when the theory is approximately conformal, or scale-invariant [78]. In this case, the $U(1)$ symmetry is broken dynamically through the Coleman–Weinberg mechanism [79] and the small deviation from scale-invariance implies a suppression of the transition probability, and generically a large amount of supercooling [80]. As such, bubble collisions take place in the vacuum, which increases the duration of the PT, thus enhancing the amplitude of the corresponding GW signal [70, 71, 81].¹

¹See, for instance, Refs. [82–94] for exploitations of this mechanism in other BSM contexts. This has also been used in the context of baryogenesis via leptogenesis [95–97], complementarity with collider searches [98]

Analyzing the rich cosmological implications of such supercooled PTs for ALPs is the main objective of this work. In particular, we show that, besides an enhanced GW signal, a supercooled FOPT also leads to the formation of primordial black holes (PBHs) through the collapse of bubbles of false vacuum. In the past years, several mechanisms have been proposed regarding the formation of PBHs in the early Universe [100]. The cosmological and astrophysical implications of PBHs can be significant [101]. In particular, sub-solar mass PBHs which are formed due to the gravitational collapse of large overdensities in the primordial plasma [102] may explain 100% of the observed DM relic density of the Universe in the PBH mass range $10^{-16}M_{\odot} \lesssim M_{\text{PBH}} \lesssim 10^{-10}M_{\odot}$ [101, 103–105], where $M_{\odot} = 2 \times 10^{33}$ g is the solar mass. Even if PBHs were so light that they Hawking-evaporated [106, 107] quickly after their formation, they might have affected the DM phenomenology [108–115]. Heavier PBHs, around solar mass scale and higher, can instead contribute to the LIGO-VIRGO GW events [116–122] or provide seeds for structure formation [123–125]. Therefore investigating formation mechanisms of such PBHs is interesting on its own.

During cosmic inflation, primordial overdensities may collapse into PBHs after re-entering the Hubble horizon in the post-inflationary period [126]. However, for single-field inflationary scenarios, the resulting PBH abundance is exponentially sensitive to the amplitude of the curvature perturbations, and therefore it requires extreme fine-tuning [127].² In this respect, other formation mechanisms such as collapsing of false vacuum bubbles, cosmic strings, domain walls or from preheating [130–133] may reduce such fine-tuning. In this work, we will focus on PBH formation from supercooled FOPTs. Although this mechanism was first suggested in the pioneering works of Refs. [134, 135], it has recently received great interest due to its successful implementation in BSM scenarios with predictable results that can be tested [136–146].

The core idea is simple: FOPTs proceed via the nucleation of bubbles of the broken phase in an initial background of the symmetric phase [147–149]. In a supercooled regime, the energy density of the Universe in the symmetric phase is dominated by the vacuum energy which acts as a cosmological constant and leads to an inflationary period. In a nucleated bubble, instead, such energy is quickly converted into radiation and the corresponding patch expands much slower. Since bubble nucleation is a stochastic phenomenon, and since, in a supercooled regime, regions outside the nucleated bubbles expand much faster than those inside, a delayed nucleation within a causal patch can develop a large overdensity that eventually collapses, if large enough, into a PBH. The production mechanism of PBHs by such “late-time blooming” during strong FOPTs, was first studied in Refs. [135, 150–154], but has recently received a lot of attention [139, 141, 144, 155–162], also in connection to the PTA signals observed in the form of a SGWB [28, 163–165]. We will study the formation of PBHs from supercooled FOPT in an explicit ALP realization, where there are only two relevant free parameters, namely, the ALP decay constant f_a and a non-Abelian gauge coupling g . This makes the model very predictive.

We find that the mass of the PBH scales with the square of the inverse power of f_a . Depending on f_{PBH} , the fraction of DM in the form of PBHs today, the PBH mass is constrained over a large range, from $10^{-24} M_{\odot}$ (corresponding to $f_a \sim 10^{12}$ GeV), excluded by evaporating PBHs during Big Bang Nucleosynthesis (BBN), to $10^5 M_{\odot}$ (corresponding to $f_a \sim 10^{-2}$ GeV), excluded by CMB accretion, with an allowed window $10^{-16}M_{\odot} \lesssim M_{\text{PBH}} \lesssim 10^{-10}M_{\odot}$

and of the generation of the Planck scale [99].

²Fine-tuning may be reduced by introducing poles in the inflaton kinetic term [128] or in the presence of spectator fields during inflation [129].

where $f_{\text{PBH}} = 1$ (100% DM). The f_{PBH} , on the other hand, is mainly controlled by the inverse time duration of the PT, which is related to the tunneling rate β/H (where H is the Hubble expansion rate). For values of $\beta/H \sim 5 - 7$, the PBH population can explain the entire DM. If the amount of supercooling is larger, namely for smaller values of β/H , the formation of PBHs can, instead, quickly overclose the Universe.

We show that the constraint from the overproduction of PBHs, as well as the bounds on their mass from BBN, CMB and microlensing [166], can strengthen the interplay between GW searches and laboratory, astrophysical and cosmological constraints on the ALP decay constant f_a [167]. Through this three-pronged complementarity, we are able to severely cut down the allowed ALP parameter space. Specifically, the GW sensitivity reach of future interferometers and the PBH parameter space ruled out by the aforementioned constraints can be directly mapped onto the ALP parameter space, which provides new bounds on ALP couplings. Conversely, depending on the strength of ALP interactions to SM particles, the bound on the ALP decay constant can be translated into a lower bound on the PBH mass scale. As a side note, we also show that the recent NANOGrav signal of stochastic GW in the nHz frequency range can be explained in our model with $f_a \simeq (10 \text{ GeV} - 1 \text{ TeV})$ and $g \simeq 0.56 - 0.60$; however, in the simplest realization, this falls in the PBH overclosure region ($f_{\text{PBH}} > 1$).

The rest of this article is organized as follows: in Section 2 we discuss supercooled PT in the ALP scenario, provide an explicit realization and identify the parameter space responsible for supercooling due to radiative symmetry breaking. In Section 3, we discuss the predictions for the GW signal. In Section 4, we discuss the PBH formation. In Section 5 we present our numerical results. In Section 6 we show the three-pronged complementarity of ALP phenomenology following PBH, GW and laboratory/astrophysical searches. Our conclusions are given in Section 7. Some supplementary plots for $f_{\text{PBH}} \ll 1$ are given in Appendix A.

2 The supercooled ALP phase transition

We consider a scenario with spontaneous radiative breaking of a global $U(1)$ symmetry [168]. To realize this scenario, we consider a collection of massless scalars, some of which charged under the $U(1)$ symmetry, described by the tree level potential

$$V(\phi) = \frac{\lambda_{ijkl}}{4} \phi_i \phi_j \phi_k \phi_l. \quad (2.1)$$

As shown in Ref. [168], the renormalization group equations of the quartic couplings generically imply that a linear combination of those vanishes at some energy scale Λ . At that scale, one can identify a flat direction in the potential parameterized by a unit vector \vec{n} . In the field coordinates $\vec{\phi} = \vec{n}\sigma$, the tree-level potential vanishes identically in the direction of σ . As such, the dynamics of the system along σ is fully controlled by the one-loop radiative corrections and the effective potential can be recast in the form

$$V_{\text{eff}}(\sigma) = \frac{\beta_{\lambda_{\text{eff}}}}{4} \sigma^4 \left(\log \frac{\sigma}{f} - \frac{1}{4} \right), \quad (2.2)$$

where $\beta_{\lambda_{\text{eff}}}$ is the β function of the effective quartic coupling $\lambda_{\text{eff}}(\mu) = \lambda_{ijkl}(\mu) n_i n_j n_k n_l$ satisfying the condition $\lambda_{\text{eff}}(\Lambda) = 0$. For positive $\beta_{\lambda_{\text{eff}}}$, the effective potential has a minimum at f and the σ field acquires a mass $m_\sigma^2 = \beta_{\lambda_{\text{eff}}} f^2$.

2.1 Finite-temperature effects

Around the origin, $\sigma \simeq 0$, the potential V_{eff} is flat (since the second-order derivative is vanishing) and the finite temperatures effects become extremely relevant [80], inducing a quadratic positive curvature for any $T > 0$, thus effectively turning the local maximum at $\sigma = 0$ into a local metastable minimum. These thermal effects are described by the finite-temperature potential

$$V_T(\sigma, T) = \frac{T^4}{2\pi^2} \sum_{\text{b}} J_B \left(\frac{m_{\text{b}}^2(\sigma)}{T^2} \right) + \frac{T^4}{2\pi^2} \sum_{\text{f}} J_F \left(\frac{m_{\text{f}}^2(\sigma)}{T^2} \right), \quad (2.3)$$

where $m_{\text{b},\text{f}}(\sigma)$ are the field-dependent masses of all the relevant bosonic and fermionic fields, and $J_{B,F}$ are the corresponding thermal functions given by

$$J_{B/F}(y^2) = \int_0^\infty dt t^2 \log \left[1 \mp \exp \left(-\sqrt{t^2 + y^2} \right) \right]. \quad (2.4)$$

Near the origin, due to the vanishing of the second-order derivative, the high-temperature expansion ($y^2 \ll 1$) is always well-justified. In this limit, the free-energy of the system along the σ direction can be written as ³

$$F(\sigma, T) \simeq -\frac{\pi^2}{90} g_* T^4 + a \frac{T^2}{24} \sigma^2 + \frac{\beta_{\lambda_{\text{eff}}}}{4} \sigma^4 \left(\log \frac{\sigma}{f} - \frac{1}{4} \right) + V_0 \quad (2.5)$$

where $g_* = N_{\text{b}} + \frac{7}{8} N_{\text{f}}$ represents the effective number of relativistic degrees of freedom in the meta-stable phase, the coefficient a is defined as $a\sigma^2 \equiv [\sum_{\text{b}} m_{\text{b}}^2(\sigma) + \frac{1}{2} \sum_{\text{f}} m_{\text{f}}^2(\sigma)]$ and V_0 , given by $V_0 = -V_{\text{eff}}(\sigma = f) = \beta_{\lambda_{\text{eff}}} f^4/16$, is chosen to remove the cosmological constant in the global minimum.

Away from the origin, the high-temperature expansion used above is valid provided that $\sigma \lesssim T/\hat{g}$ with \hat{g} being the typical coupling constant in the field-dependent mass $m(\sigma) \sim \hat{g}\sigma$. During a supercooled PT, the free-energy above can be further simplified by noting that

$$\log \frac{\sigma}{f} = \log \frac{\hat{g}\sigma}{T} + \log \frac{T}{\hat{g}f} \simeq \log \frac{T}{\hat{g}f} \equiv \log \frac{T}{M}, \quad (2.6)$$

with M being the typical heavy mass scale at the minimum. Indeed, while during supercooling $T \ll M$, the bounce action will get much of its contribution from field values around the barrier, for which $\hat{g}\sigma/T \sim 1$. In this case the free-energy can be recast in a simple polynomial form with a positive quadratic and a negative quartic term⁴

$$F(\sigma, T) \simeq \frac{m^2(T)}{2} \sigma^2 - \frac{\lambda(T)}{4} \sigma^4 \quad (2.7)$$

with $m^2(T) = aT^2/12$, $\lambda(T) = \beta_{\lambda_{\text{eff}}} \log(M/T)$ and the field-independent terms omitted here are irrelevant for the computation of the transition rate.

³Bosonic degrees of freedom also provide a cubic term in the m^2/T^2 expansion which has a mild numerical impact on the computation of the temperature-dependent bounce action in supercooled PTs [70, 169].

⁴We can check a posteriori the validity of the approximation by noting that the potential in Eq. (2.7) provides a barrier size $\sigma_b = \sqrt{2m^2(T)/\lambda(T)} = T\sqrt{a/(6\beta_{\lambda_{\text{eff}}}\log(M/T))} < T/\hat{g}$ due to the large logarithm.

The PT of the model in Eq. (2.7) is controlled by the 3-D bounce action $S_3/T \approx 18.897 m(T)/(\lambda(T)T) \equiv A_3/\log(M/T)$, which depends only logarithmically on the temperature as a result of the approximate scale invariance of the model. The corresponding tunneling rate is given by

$$\Gamma \simeq T^4 \left(\frac{S_3}{2\pi T} \right)^{\frac{3}{2}} \exp(-S_3/T), \quad (2.8)$$

and the slow (logarithmic) temperature dependence in the bounce action generically implies a phase of supercooling. Beside tunneling at finite temperature, nucleation of true vacuum bubbles can also be driven by 4-D bounces. If the $O(4)$ bounce action S_4 is smaller than S_3/T , quantum effects can lead to a faster nucleation rate but we find that the thermal nucleation rate always dominates in the relevant regions of our parameter space.

The nucleation temperature is defined by $\Gamma/H^4 = 1$, with the Hubble rate given by

$$H^2 = \frac{1}{3M_{\text{Pl}}^2} \left[\frac{\pi^2}{30} g_* T^4 + V_0 \right] \simeq \frac{V_0}{3M_{\text{Pl}}^2} \equiv H_I^2, \quad (2.9)$$

where $M_{\text{Pl}} = 2.4 \times 10^{18}$ GeV is the reduced Planck mass, and the right-hand side of Eq. (2.9) holds during the supercooling phase, under which the Universe becomes vacuum-dominated and experiences an inflationary period. Using the equation above, the nucleation temperature is found to be

$$T_n \simeq \sqrt{MH_I} \exp \left(\frac{1}{2} \sqrt{-A_3 + \log^2(M/H_I)} \right), \quad (2.10)$$

with a lower bound given by $T_n^{\text{min}} = \sqrt{MH_I} \simeq 0.1 f(f/M_{\text{Pl}})^{1/2}$.

The strength α of the PT can be characterized by the free energy difference between the metastable and true vacua, normalised to the radiation density. During supercooling, the vacuum energy dominates and we have

$$\alpha = \frac{1}{\rho_{\text{rad}}} \left(1 - T \frac{\partial}{\partial T} \right) \left[F(0, T) - F(\sigma_n, T) \right] \Big|_{T_n} \simeq \frac{V_0}{\rho_{\text{rad}}(T_n)} = \left(\frac{T_{\text{inf}}}{T_n} \right)^4, \quad (2.11)$$

with $T_{\text{inf}} = (30V_0/(g_*\pi^2))^{1/4}$ being the temperature at which the Universe becomes vacuum-dominated.⁵

Finally, the logarithmic derivative of the tunneling rate is found to be

$$\frac{\beta}{H} = - \frac{d \log \Gamma}{d \log T} \Big|_{T=T_n} \simeq -4 + T \frac{d(S_3/T)}{dT} \Big|_{T=T_n} = -4 + \frac{A_3}{\log^2(M/T_n)}, \quad (2.12)$$

which clearly shows that, in the supercooling regime, β/H can become of order $O(1)$ thus maximizing the power spectrum of GW as well as the production of PBHs.

After the completion of the PT the Universe is reheated at a temperature

$$T_{\text{RH}} = T_{\text{inf}} \min \left(1, \frac{\Gamma}{H_I} \right)^{1/2}, \quad (2.13)$$

where Γ is the relevant decay rate into the SM plasma. For the sake of simplicity, in the following we will assume sufficiently fast reheating, namely $T_{\text{RH}} \simeq T_{\text{inf}}$.

Within the approximations discussed above, the dynamics is controlled by the three parameters f , $\beta_{\lambda_{\text{eff}}}$ and a (see also Ref. [169]) which can be completely specified once an explicit realization of the model is provided.

⁵We assume that g_* does not change between T_{inf} and T_n .

2.2 An explicit ALP realization

As a prototype for an elementary realization of the radiative breaking of the global $U(1)$ symmetry, let us consider a pair of complex scalar fields ϕ_1 and ϕ_2 , neutral under the SM gauge group, a pair of vector-like fermions ψ, ψ^c , and an $SU(2)$ gauge field A^μ , with gauge coupling g . Under the new $SU(2)$ symmetry only ϕ_1 is charged, while being neutral under the global $U(1)$. The ϕ_2 transforms, instead, under the global $U(1)$ and its phase corresponds to the ALP. The $SU(2)$ gauge sector controls the running of the effective quartic coupling of the scalar potential. The simpler choice of an abelian gauge group would have worked equally well. We opted for the non-abelian scenario to avoid possible issues associated to the Landau pole and further complications related to the presence of cosmic strings. The latter might actually enrich the phenomenology of the model and their interplay will be addressed in a separate work.

The Lagrangian of the model is given by

$$\mathcal{L} = -\frac{F^2}{4g^2} + |D_\mu \phi_1|^2 + |\partial_\mu \phi_2|^2 + (y\phi_2\psi\psi^c + \text{h.c.}) - \lambda_1|\phi_1|^4 - \lambda_2|\phi_2|^4 - \lambda_{12}|\phi_1|^2|\phi_2|^2 \quad (2.14)$$

where $F^{\mu\nu}$ and D^μ are the field strength and the covariant derivative of the $SU(2)$ gauge field, respectively. For the sake of simplicity, in order to disentangle the radiative global $U(1)$ breaking from the electroweak symmetry breaking, we neglect the tree-level portal couplings to the SM Higgs doublet. This class of models has been studied in Refs. [70, 71] in the context of supercooled QCD-axion models and similar realizations were also addressed in the context of electroweak PTs in Refs. [85, 170, 171]. Another interesting scenario is characterized by a composite ALP arising from the spontaneous breaking a global symmetry of a strongly coupled dynamics. In this context, a supercooled PT can be realized within a strongly coupled conformal sector with the spontaneous breaking of scale invariance [70, 71]. For the sake of definiteness, in this paper we focus on an elementary ALP scenario.

In the potential of Eq. (2.14), the flat direction of the tree-level potential is found at a scale Λ at which $\lambda_{12} = -2\sqrt{\lambda_1\lambda_2}$ and, in the manifold of the scalar fields, is parameterized by

$$\phi_i = (\cos \theta, \sin \theta) \frac{\sigma}{\sqrt{2}}, \quad \text{with} \quad \tan^2 \theta = \sqrt{\frac{\lambda_1}{\lambda_2}}. \quad (2.15)$$

Along the flat direction σ , the field-dependent masses of the gauge field A^μ , the fermion ψ and the scalar field τ in the radial direction orthogonal to σ are respectively given by

$$M_A = g \cos \theta \sigma, \quad M_\psi = \frac{y}{\sqrt{2}} \sin \theta \sigma, \quad M_\tau = (4\lambda_1\lambda_2)^{1/4} \sigma. \quad (2.16)$$

In the previous list we did not count the phase of ϕ_2 , the ALP, being exactly massless at this level, and the σ , the mass of which is loop-suppressed. With the rotation angle θ introduced in Eq. (2.15), the axion decay constant f_a is given by $f_a = f \sin \theta$. The effective potential in the direction of σ takes the form of V_{eff} in Eq. (2.2) with

$$\beta_{\lambda_{\text{eff}}} = \frac{\partial \lambda_{\text{eff}}}{\partial \log \mu} = \frac{1}{16\pi^2} [6Ng^4 \cos^4 \theta - 2y^4 \sin^4 \theta + 8\lambda_1\lambda_2], \quad (2.17)$$

where $N = 3$ is the number of gauge bosons of $SU(2)$. Analogously, we can compute the thermal corrections and, in particular, we can extract the coefficient of the quadratic terms

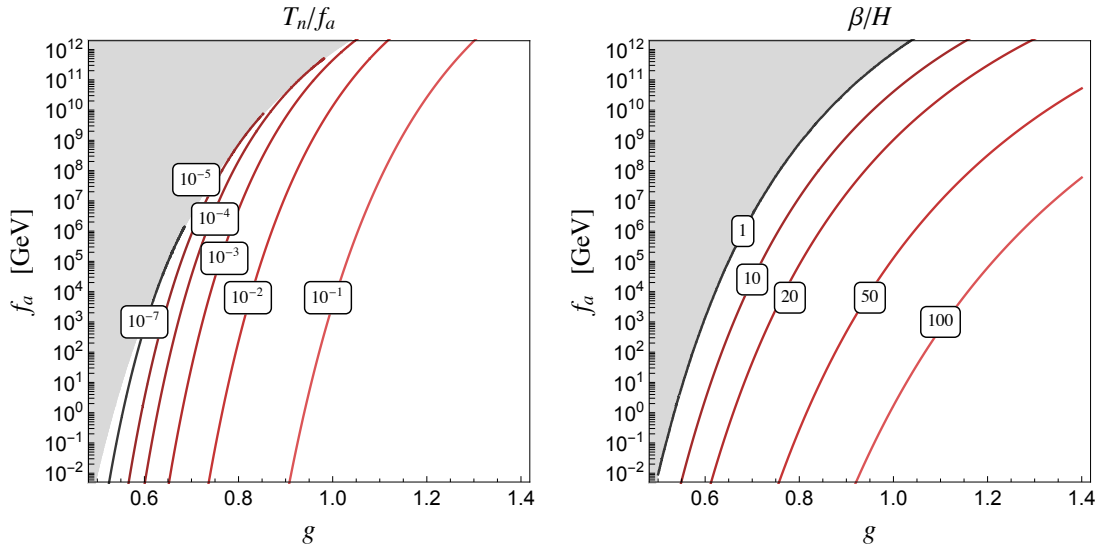


Figure 1. Contours showing the nucleation temperature T_n (in units of f_a) and the β/H parameter in the plane of the model parameters f_a and g . In the gray region nucleation never occurs.

in high-temperature regime:

$$a = 3Ng^2 \cos^2 \theta + 3y^2 \sin^2 \theta + 2\sqrt{\lambda_1 \lambda_2}. \quad (2.18)$$

In the following, we will address the scenario in which the gauge coupling dominates, namely, $\lambda_1 \simeq \lambda_2 \ll g^2$ and $y \simeq 0$.

In Fig. 1 we show the contours of the nucleation temperature (left panel) and the β/H parameter (right panel) in the parameter space of the model discussed here, entirely defined by the gauge coupling g and the axion decay constant f_a . In the present work, we focus on the supercooling regime, approximately determined by $T_n/f_a \lesssim 10^{-2}$. In this case, the dependence of T_n , β/H and α is well described by the analytic approximations discussed in Section 2.1. In the supercooling regime, α is always very large, $\alpha \gg 1$, and basically drops out from the expressions of both the GW spectrum and the PBH abundance that will be discussed below. For this reason, we do not show the dependence of α .

In the gray region of Fig. 1, the system remains stuck in the inflationary phase. Nevertheless, the de Sitter fluctuations in the false vacuum may actually push the field into the true ground state, thus effectively completing the transition. This happens when the Hubble constant becomes larger than the height of the barrier. To describe this process, one should take into account the de Sitter curvature [172, 173] in the computation of the tunneling rate. We do not address this case in our work, and will therefore stick to the unshaded region of parameter space in Fig. 1.

3 GW signals from supercooled ALP phase transition

The spectra for GW signal is as usual given by

$$h^2 \Omega_{\text{GW}}(f) \equiv \frac{h^2}{\rho_c} \frac{d\rho_{\text{GW}}}{d \log f} \quad (3.1)$$

where ρ_{GW} is the energy density in GWs, ρ_c is the critical density of the Universe, and h is the dimensionless Hubble parameter. After the GWs are produced in the early Universe they are red-shifted and we observe them today with an amplitude [174]

$$h^2 \Omega_{\text{GW}} = h^2 \Omega_{\text{rad}}(T_0) \left(\frac{g_{*s}(T_0)}{g_{*s}(T_{\text{RH}})} \right)^{1/3} \Omega_{\text{GW}*} \quad (3.2a)$$

$$= \frac{g_*(T_0) \pi^2 T_0^4}{30} \frac{1}{3H_{100}^2 M_{\text{Pl}}^2} \left(\frac{g_{*s}(T_0)}{g_{*s}(T_{\text{RH}})} \right)^{1/3} \Omega_{\text{GW}*} \quad (3.2b)$$

$$= 6.56 \times 10^{-5} (g_{*s}(T_{\text{RH}}))^{-1/3} \Omega_{\text{GW}*}, \quad (3.2c)$$

where we used $\Omega_{\text{rad}}(T_{\text{RH}}) \equiv \rho_{\text{rad}}/\rho_c = 1$ just after the FOPT and $\Omega_{\text{GW}*}$ is the GW signal just after the PT, $T_0 \simeq 0.23$ meV is the CMB temperature today, and $H_{100} \equiv 100$ km/s/Mpc. Similarly, the frequency is also red-shifted as

$$f_0 = \left(\frac{g_{*s}(T_0)}{g_{*s}(T_{\text{RH}})} \right)^{1/3} \frac{T_0}{T_{\text{RH}}} f_*, \quad (3.3)$$

with f_* denoting the frequency of the GW spectrum at the PT. The reheating that occurs at the end of the FOPT is characterized by the temperature, via the first Friedmann equation:

$$T_{\text{RH}} = \left(\frac{90 M_{\text{Pl}}^2 H(T_{\text{RH}})^2}{g_*(T_{\text{RH}}) \pi^2} \right)^{1/4}. \quad (3.4)$$

Notice also that, for supercooled PTs, we will deal with highly relativistic bubble walls.

For the estimates of the spectral shape of GWs from a FOPT we use the results from the hybrid simulations obtained in Ref. [175] in which the anisotropic stress induced in a bubble collision was first determined in a (1+1)-dimensional simulation. The interesting aspect of the analysis is that there are notable differences in the GW spectra between non-gauged and gauged scenarios (see Ref. [176] for the non-gauged case and Ref. [175] for the gauged case of U(1) symmetry breaking⁶). Since we have a gauged theory, the GW spectrum is characterized by

$$h^2 \Omega_{\text{hyb}}(f) = 5.10 \times 10^{-9} \left(\frac{100}{g_*(T_{\text{RH}})} \right)^{1/3} \left(\frac{10}{\beta_H} \right)^2 S_{\text{hyb}}(f), \quad (3.5)$$

with the shape,

$$S_{\text{hyb}}(f) = \frac{695}{\left[2.41 \left(\frac{f}{\tilde{f}_{\text{hyb}}} \right)^{-0.557} + 2.34 \left(\frac{f}{\tilde{f}_{\text{hyb}}} \right)^{0.574} \right]^{4.20}}, \quad (3.6)$$

and peak frequency

$$\tilde{f}_{\text{hyb}} = 1.1 \times 10^{-4} \text{ Hz} \left(\frac{g_*}{100} \right)^{1/6} \left(\frac{\beta_H}{10} \right) \left(\frac{T_{\text{RH}}}{500 \text{ GeV}} \right). \quad (3.7)$$

The expressions above are only valid for the FOPT we are interested in, that is supercooled PT. This basically means we are considering the limit $\alpha \gg 1$, and ultra-relativistic bubble-wall velocity $v_w \simeq 1$.

⁶Simulation with non-Abelian gauge theory has not been done; however, we do not expect much to change as the GW spectrum varies very mildly and does not impact our analysis too much.

Other estimates of the GW spectral shapes are available in the literature, e.g. the one obtained using $(3 + 1)$ -dimensional lattice simulations of thick wall bubble collisions [177] and the semi-analytical estimates developed in Refs. [178, 179]. We checked that all these estimates provide similar results after requiring the correct scaling $h^2\Omega_{\text{GW}} \sim f^3$ for super-horizon modes [180–184].

4 PBH formation from supercooled ALP phase transition

PBHs can be formed due to the collapse of overdense regions during a strong FOPT [139, 144, 158, 159]. During a supercooled PT, when the plasma temperature reaches T_{inf} , the Universe enters a vacuum-dominated era and a phase of inflation takes place. This period lasts until T_n , when bubble nucleation becomes efficient. Then, regions of the Universe undergo a transition to the true ground state and get reheated at $T_{\text{RH}} \simeq T_{\text{inf}}$. Since nucleation is a stochastic process, some Hubble patches may remain in the false vacuum and inflate more.

When bubble nucleation begins, and afterwards during bubble growth, the vacuum energy is converted into energy stored in the bubble wall, energy dumped into the plasma and sound waves from bubble collisions, all of them redshifting away as radiation, decreasing as $\propto a^{-4}(t)$. On the other hand, casual patches in which nucleation is delayed still inflate due to the constant, and dominating, vacuum energy contribution. Eventually, they generate an overdensity with respect to the surrounding average background.

The ratio $\rho_{\text{rad}}^{\text{late}}/\rho_{\text{rad}}^{\text{bkg}}$ between the energy densities of the late-blooming patch and of the background keeps increasing until it reaches a maximum value, approximately determined by the percolation temperature of the former. If the overdensity of the late-nucleated patch, quantified by the density contrast $\delta = \rho_{\text{rad}}^{\text{late}}/\rho_{\text{rad}}^{\text{bkg}} - 1$, is larger than a critical threshold, usually $\delta_c \simeq 0.45$, the patch can collapse into a PBH [185] (see Refs. [139, 144, 158, 159] for more details⁷). We do not go into the details of such computations and instead follow Ref. [159] for our estimates.

The probability that a Hubble patch collapses into a PBH can be approximated, in the limit of $\alpha \gtrsim 10^2$, by the analytic formula

$$P_{\text{coll}} \simeq \exp \left[-a \left(\frac{\beta}{H_n} \right)^b (1 + \delta_c)^{c \frac{\beta}{H_n}} \right], \quad (4.1)$$

where the coefficients $a \simeq 0.5646$, $b \simeq 1.266$, $c \simeq 0.6639$ are fitted from a numerical computation. The collapsing probability does not depend on the scale of the PT, but only on the β/H_n parameter and on the critical threshold δ_c .

The mass of the PBH is given by the energy contained within the sound horizon $c_s H^{-1}$ at the time of the collapse t_{coll} [186]:

$$M_{\text{PBH}} = k \frac{4\pi}{3} c_s^3 H^{-3} \rho_{\text{rad}}^{\text{late}} \Big|_{t_{\text{coll}}} \simeq 3.7 \times 10^{-8} M_{\odot} \left(\frac{106.75}{g_*(T_{\text{RH}})} \right)^{1/2} \left(\frac{500 \text{ GeV}}{T_{\text{RH}}} \right)^2. \quad (4.2)$$

Here $k (\leq 1)$ is a numerical factor which depends on the details of the gravitational collapse involved in such a process and M_{\odot} is the solar mass.

⁷There are minor differences in estimation of nucleation time between the studies in Ref. [139, 144, 158, 159] based on contribution from past light cones which may lead to slightly varied abundances of PBHs.

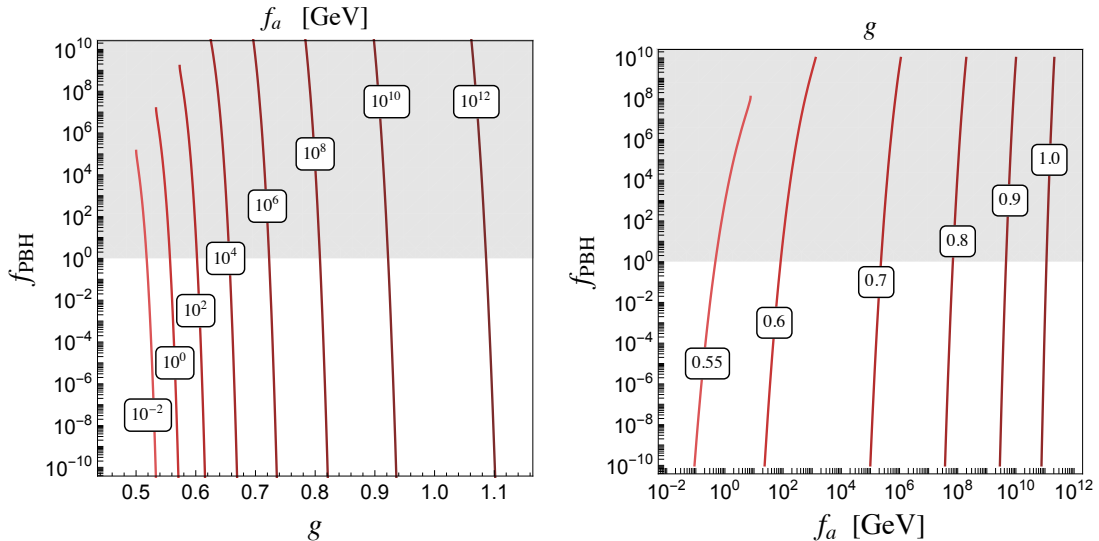


Figure 2. The fraction of DM in the form of PBH, f_{PBH} , as functions of the two parameters of the model, g (left panel) and f_a (right panel), with constant contours of the other parameter shown. The gray region corresponds to PBH overclosure.

Finally, the fraction of DM in the form of PBHs today is found to be

$$f_{\text{PBH}} \equiv \frac{\rho_{\text{PBH},0}}{\rho_{\text{DM},0}} = P_{\text{coll}} \frac{M_{\text{PBH}} \mathcal{N}_{\text{patches}}}{\frac{4\pi}{3} H_0^{-3} \rho_{\text{DM},0}} \simeq \left(\frac{P_{\text{coll}}}{6.2 \times 10^{-12}} \right) \left(\frac{T_{\text{RH}}}{500 \text{ GeV}} \right) \quad (4.3)$$

where $\rho_{\text{DM},0} \simeq 0.26 \times 3M_{\text{pl}}^2 H_0^2$ is the current DM energy density and $\mathcal{N}_{\text{patches}}$ represents the number of Hubble patches, when the temperature was T_{RH} , in our past light-cone, namely,

$$\mathcal{N}_{\text{patches}} = \left(\frac{a_{\text{RH}} H_{\text{RH}}}{a_0 H_0} \right)^3 \simeq 5.3 \times 10^{40} \left(\frac{g_*(T_{\text{RH}})}{100} \right)^{1/2} \left(\frac{T_{\text{RH}}}{500 \text{ GeV}} \right)^3. \quad (4.4)$$

The PBH abundance is shown in Fig. 2 as functions of the two parameters of the model, f_a and g .

The overdense regions generated from the late decay of the false vacuum in a super-cooled FOPT also produce curvature perturbations [187]. These can be described assuming a Gaussian distribution. If the distribution deviates from monochromaticity, the collapsing region can have a non-zero spin, although typically small for a FOPT. Despite that, it is still interesting to assess the initial spin since several mechanisms responsible for its growth after PBH formation have been explored [188–190].

The spin of the PBH can be estimated using the peak theory formalism [191, 192] and is parameterized by the dimensionless Kerr parameter a_* . Its variance can be approximated by [162, 193]

$$\langle a_*^2 \rangle^{1/2} \simeq 4.01 \times 10^{-3} \frac{\sqrt{1 - \gamma^2}}{1 + 0.036 \left[21 - 2 \log_{10} \left(\frac{f_{\text{PBH}}}{10^{-7}} \right) - \log_{10} \left(\frac{M_{\text{PBH}}}{10^{15} g} \right) \right]}, \quad (4.5)$$

and expressed in terms of the PBH mass and abundance. The parameter γ is defined in terms of the first three spectral moments of the distribution of the curvature perturbations.

Its deviation from unity describes the non-monochromaticity of such distribution. The parameter γ typically ranges in $(0.85, 1)$ [192, 193]. In the following we use a reference value of $\gamma \simeq 0.96$ [193].

5 Numerical results

In this section, we present our numerical results for the GW signal and PBH fraction in the ALP model under consideration and point out the complementarity with existing ALP and PBH constraints.

5.1 GW-PBH complementarity

In Fig. 3 we show the parameter space of the ALP model projected onto the plane defined by the gauge coupling constant g and the ALP decay constant f_a . In this plane we show contour lines of several values of β/H . As already discussed above, in the gray region in the top left corner of the plot, the transition to global minimum never occurs and the system remains trapped in the inflating regime.

We also show the contours of $\alpha = 10^2$ and $\alpha = 1$, the latter approximately identifying the boundary of the region in which supercooling is not realized. In this portion of the parameter space (gray shaded region on the bottom right corner), totally irrelevant for the purpose of our work, our prediction for the GW spectra cannot be trusted as they all rely on the supercooling hypothesis.

The three purple dashed lines delineate the values of f_a and g for which the fraction of DM in PBHs is equal to $f_{\text{PBH}} = 10^{10}, 1, 10^{-10}$, exemplifying, respectively, an overabundant PBH scenario, one in which the distribution of PBHs can exactly explain the DM relic, and an underabundant PBH case. The $f_{\text{PBH}} = 1$ case is characterized by values of $\beta/H \sim 5 - 7$, and the region above it is shown as hatched. In the slice of the plot defined by $10^{-10} < f_{\text{PBH}} < 1$, we report the constraints, given by shaded cyan regions, from the PBH searches that we will be detailed below. Concurrently, we highlight in red, on top of the $f_{\text{PBH}} = 1$ curve, the PBH mass window compatible with all the PBH bounds (see Section 5.4). This is realized by $\beta/H \sim 6.5 - 7$. See Fig. 4 for a zoomed-in view of this region.

The horizontal gray band for $f_a \lesssim 100$ MeV is excluded by the requirement that, at the end of the PT, the plasma is reheated to a temperature well above the one at which BBN occurs. In particular, we enforce the conservative bound $T_{\text{RH}} > 10$ MeV.

Finally, we consider the effective dark radiation bounds during BBN and CMB decoupling. In particular, the energy density of the primordial GW has to be smaller than the limit on dark radiation encoded in ΔN_{eff} from BBN and CMB observations since the gravitons behave as massless radiation degrees of freedom. Any change of the number of effective relativistic degrees of freedom (N_{eff}) at the time of recombination is set by [2]

$$\int_{f_{\text{min}}}^{\infty} \frac{df}{f} \Omega_{\text{GW}}(f) h^2 \leq 5.6 \times 10^{-6} \Delta N_{\text{eff}}. \quad (5.1)$$

While the lower limit for the integration is $f_{\text{min}} \simeq 10^{-10} \text{Hz}$ for BBN and $f_{\text{min}} \simeq 10^{-18} \text{Hz}$ for the CMB bounds, in practice, when we plot *e.g.* several GW spectra simultaneously, as a first-order estimate we may use the approximation to ignore the frequency dependence and to set bounds just on the energy density of the peak for a given GW spectrum; this is given by

$$\Omega_{\text{GW}}^{\text{Peak}} h^2 \leq 5.6 \times 10^{-6} \Delta N_{\text{eff}}. \quad (5.2)$$

We consider the constraints on ΔN_{eff} from BBN and the PLANCK 2018 limits [194], as well as future reaches of CMB experiments such as CMB-S4 [195, 196], CMB-Bharat [197] and CMB-HD [198, 199]. We find that the only relevant constraint can be enforced by CMB-HD around $\beta/H \lesssim 2$ and close to the separation boundary from the region in which the FOPT never completes.

In the plot, the expected sensitivity reaches of several current and future GW observatories are shown. These can be broadly classified as:

- **Ground-based interferometer detectors:** aLIGO/aVIRGO (red dashed) [35, 36, 200], AION [9] (orange solid), EINSTEIN TELESCOPE (ET) [17, 201] (blue solid), COSMIC EXPLORER (CE) [18, 202] (blue dashed).
- **Space-based interferometer detectors:** LISA [12, 203] (pink solid), BBO [16, 204] (green dashed), DECIGO/U-DECIGO [15, 205] (green solid), AEDGE [10, 206] (orange dashed), μ -ARES [11] (magenta dashed).
- **Recast from astrometry proposals (star surveys):** GAIA/THEIA [7] (brown dashed).
- **Pulsar timing arrays:** SKA [6] (purple), EPTA [207, 208] (purple dashed), NANOGrav [23] (blue shaded region).

The only existing bound comes from the SGWB search by the LIGO-VIRGO collaboration [5], as shown by the red shaded region. Also shown is the projected sensitivity at the end of the next phase, advanced LIGO-VIRGO [35, 36, 200], which is already close to the region of the parameter space relevant for PBH production. The future Einstein Telescope and LISA interferometers will probe the space in which PBH from a supercooled FOPT can explain all the observed DM abundance.

In the bottom left corner of Fig. 3, we show the 2σ region corresponding to the recent detection by the NANOGrav collaboration [23] under the hypothesis that the observed SGWB originates from a PT. The region is obtained by minimizing the following figure of merit:

$$\chi^2 = \sum_i^N \frac{(\log_{10} \Omega_{\text{th}} h^2 - \log_{10} \Omega_{\text{exp}} h^2)^2}{\sigma_i^2}, \quad (5.3)$$

where $\Omega_{\text{th}} h^2$ and $\Omega_{\text{exp}} h^2$ represent, respectively, the GW relic from our theoretical prediction of the supercooled FOPT and the experimental value from NANOGrav. For the estimate of the χ^2 we ignore the uncertainty in the frequency width and just consider, for each bin, the uncertainty σ_i in the $\log_{10}(\Omega_{\text{exp}} h^2)$, which we approximate using the half-width. We see that the interpretation of the NANOGrav signal as a stochastic background of GW from a supercooled FOPT in our ALP model is disfavored since it falls within the PBH overclosure region. However, this is only true if we assume instantaneous reheating. If there is a preheating or prolonged reheating period, aided by PBH evaporation (see e.g. Ref. [209]), some (or most) of the PBH population can in principle be diluted away by the end of reheating to relax the overclosure bound and save the NANOGrav-preferred region. We postpone this discussion to a future work.

In order to extract the sensitivity regions, we exploit the analysis developed in Ref. [210] in which, from the effective noise strain S_{noise} provided by the experimental collaborations,

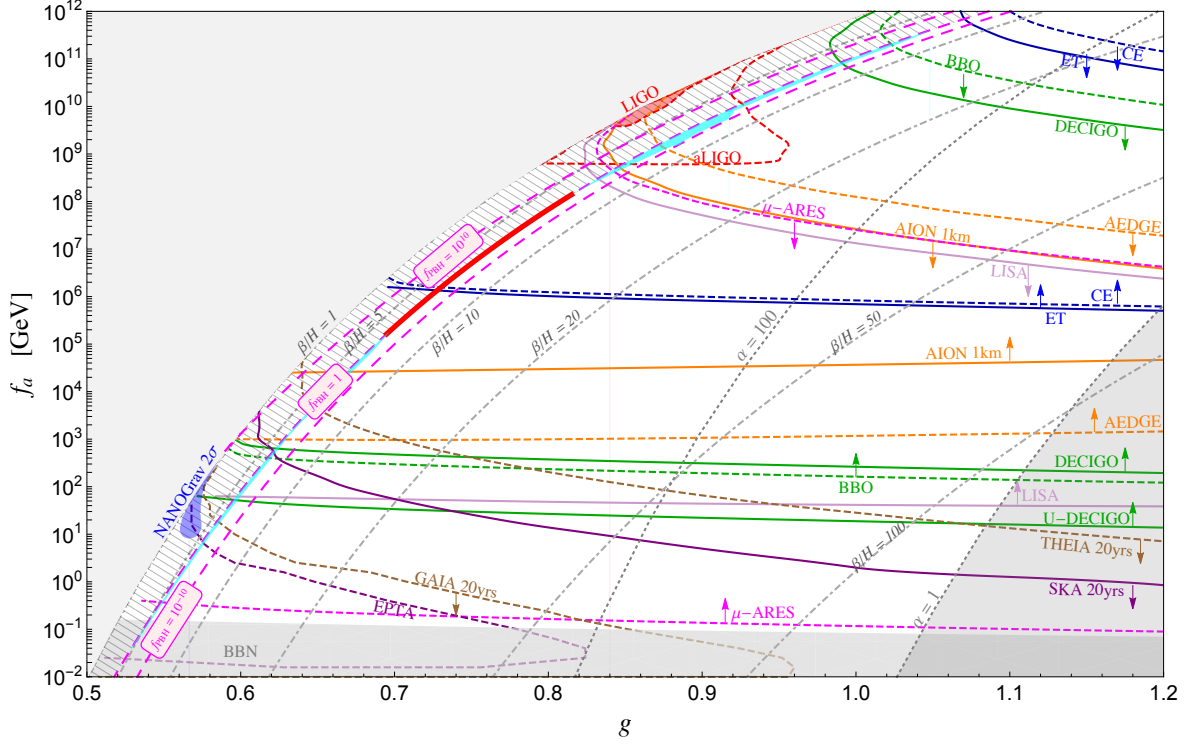


Figure 3. PBH and GW predictions in our scale-invariant $SU(2)$ realization of the ALP model. Some contours of f_{PBH} (purple), α and β/H are shown. The gray and red shaded regions are disfavored. The thick red line shows the allowed region where PBHs can explain 100% DM relic. The blue shaded region is the 2σ preferred region to explain the NANOGrav signal. Other solid/dashed lines correspond to the sensitivities of the future GW detectors. See text for further details.

we compute the power-law integrated (PLI) limit by maximizing the signal-to-noise (SNR) ratio over the spectral index. The SNR for a signal $\Omega(f_{\text{gw}})$ is defined as

$$\text{SNR} = \sqrt{t_{\text{obs}} \int_{f_{\text{min}}}^{f_{\text{max}}} df \left[\frac{\Omega(f)}{\Omega_{\text{noise}}(f)} \right]^2}, \quad \Omega_{\text{noise}}(f_{\text{gw}}) = \frac{2\pi^2}{3H_0^2} f^3 S_{\text{noise}}(f_{\text{gw}}), \quad (5.4)$$

where the prefactor t_{obs} represents the integrated observational time, multiplied by the number of interferometers involved in the experiment. To determine a conservative bound, we assume a power-law family of signals $\Omega_b(f_{\text{gw}}) = A_b f_{\text{gw}}^b$ and we extract, at each frequency f_{gw} , the largest value of $\Omega_b(f_{\text{gw}})$ compatible with a given reference value of SNR_{ref} , here taken as 10. This gives the (PLI) limit

$$\begin{aligned} \Omega_{\text{PLI}}(f_{\text{gw}}) &= \max_b \Omega_b(f_{\text{gw}}) \Big|_{\text{SNR}_{\text{ref}}} = \max_b A_b \Big|_{\text{SNR}_{\text{ref}}} f_{\text{gw}}^b \\ &= \frac{\text{SNR}_{\text{ref}}}{\sqrt{t_{\text{obs}}}} \max_b \left[\left(\int_{f_{\text{min}}}^{f_{\text{max}}} df \frac{\bar{f}^{2b}}{\Omega_{\text{noise}}^2(\bar{f})} \right)^{-\frac{1}{2}} f_{\text{gw}}^b \right]. \end{aligned} \quad (5.5)$$

In Fig. 4 we show a zoomed-in version of Fig. 3 around the region in which the distribution of PBH can explain the total DM abundance ($f_{\text{PBH}} = 1$), thus emphasizing the corresponding variability range of the two microphysical parameters, g and f_a . Dashed gray

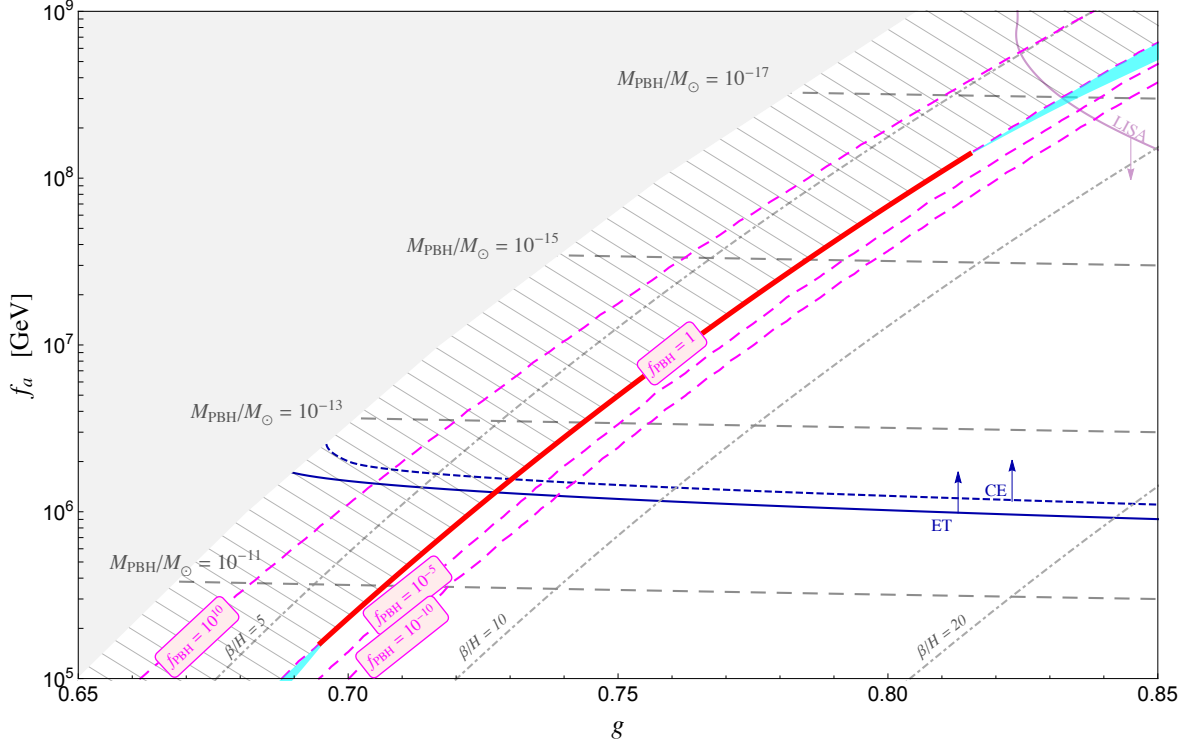


Figure 4. Same as Fig. 3 but zoomed in around the $f_{\text{PBH}} = 1$ line. Also shown are some relevant M_{PBH} contours (in units of M_{\odot}).

lines show some representative values of the PBH mass which give the correct DM relic density. As mentioned above, future GW detectors like LISA, AION, ET and CE will be able to probe this entire allowed parameter space in our ALP model.

5.2 The astrophysical foreground

As mentioned in the Introduction, the cosmological stochastic GW signal discussed here is subject to an astrophysical foreground from unresolved compact binary coalescences [211]. LIGO/VIRGO has already observed GW events involving binary black hole (BH-BH) and binary neutron stars (NS-NS) mergers [212, 213]; hence, an astrophysical foreground is guaranteed to exist. The sum of the diffuse astrophysical foreground is shown in Fig. 5 as the gray shaded region in the bottom half plane (see also Refs. [37, 128]). Different subtraction methods have been proposed to deal with this foreground at future GW detectors and to extract any potential signal of primordial origin [214–222]. We expect that the NS and BH foreground can be subtracted from the sensitivities of BBO and ET or CE in the ranges $\Omega_{\text{GW}} \simeq 10^{-15}$ [214] and $\Omega_{\text{GW}} \simeq 10^{-13}$ [216]. However in the LISA window, the galactic and extra-galactic binary white dwarf (WD-WD) foregrounds may dominate over the NS-NS and BH-BH foregrounds [223–225] and should be subtracted [226] from the expected sensitivity $\Omega_{\text{GW}} \simeq 10^{-13}$ to be reached at LISA [227, 228]. Given that such subtractions can be made possible with a network of GW detectors due to the fact that the GW spectrum generated by the astrophysical foreground increases with frequency as $f^{2/3}$ [215, 229], which is different from the GW spectrum generated by nucleating bubbles during strong FOPT ($\Omega_{\text{GW}} \sim f^{2.3}$

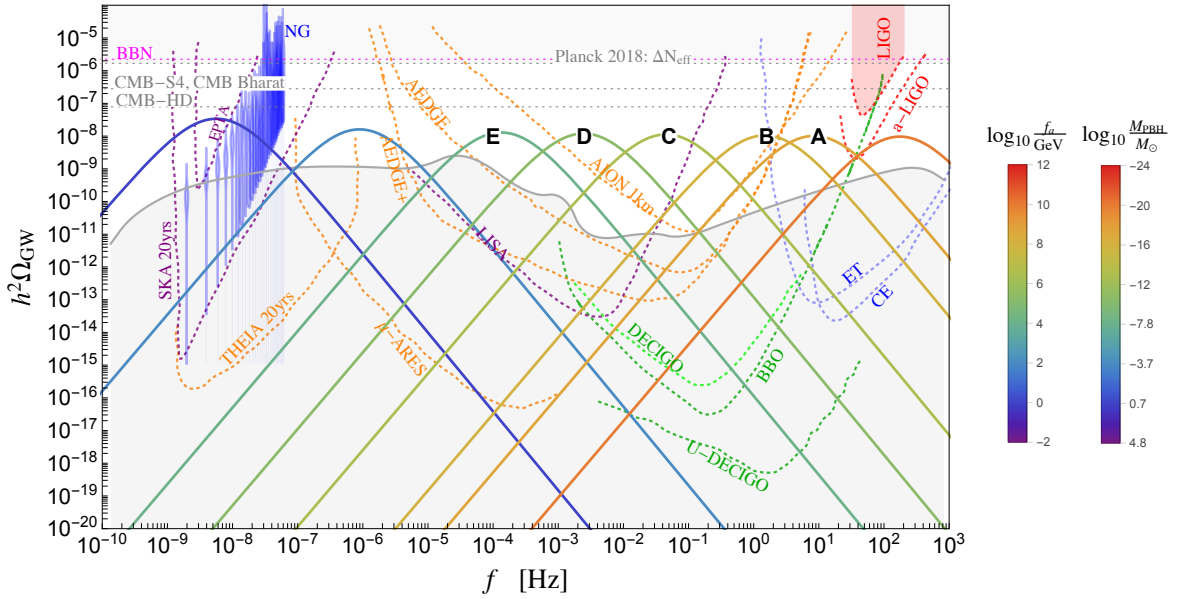


Figure 5. The GW spectra predicted in our ALP model are shown by the colored solid lines corresponding to different values of f_a , which have a one-to-one correspondence with the PBH mass (for a fixed $f_{\text{PBH}} = 1$). Five benchmark points (A to E) are marked here, which will be used later. The areas above the colored dotted lines correspond to the projected sensitivities for several current and future GW observatories. The horizontal lines show current ΔN_{eff} constraints from BBN and Planck data (shaded regions) and future reaches by CMB-S4, CMB-Bharat and CMB-HD. The red shaded region on top right is the current exclusion from LIGO-VIRGO data. The blue violins on the top left are the recent NANOGrav data points for the SGWB detection. The shaded region on the bottom half of the plane is the expected astrophysical foreground. See text for details.

and $\Omega_{\text{GW}} \sim f^{-2.4}$ for frequencies below and above the peak, respectively; see Fig. 5), we hope to be able to eventually pin down the GW signals from supercooled PT.

5.3 Fitting the NANOGrav signal

In Fig. 6, we focus on the nHz frequency regime and the 15-year NANOGrav data on the SGWB [23]. Our ALP model can explain this signal for $f_a \simeq (10 \text{ GeV} - 1 \text{ TeV})$ and $g \simeq 0.56 - 0.60$. The best-fit GW spectrum is shown by the solid orange curve and the 2σ band is shown by the dashed orange curves. For comparison, we also show the expected band of spectra from astrophysical sources, namely, supermassive black hole (SMBH) binaries [230]. Our cosmological signal tends to fit the NANOGrav data better, but a more accurate modeling of the SMBH background could alter this result. Our 2σ best-fit spectrum is also consistent with the ΔN_{eff} bound from BBN and Planck data (horizontal gray shaded region). However, as shown in Fig. 3, the required values of f_a and g in our model to fit the NANOGrav signal lead to PBH overproduction, and thus, disfavored in the simplest version.

5.4 PBH constraints

In Fig. 7 we depict the observational constraints on f_{PBH} (see Ref. [105] for a review). PBH evaporation via Hawking radiation give constraints in (see also Refs. [231–233]): CMB [234], EDGES [235], INTEGRAL [236, 237], Voyager [238], 511 keV [239], and EGRB [240]. The

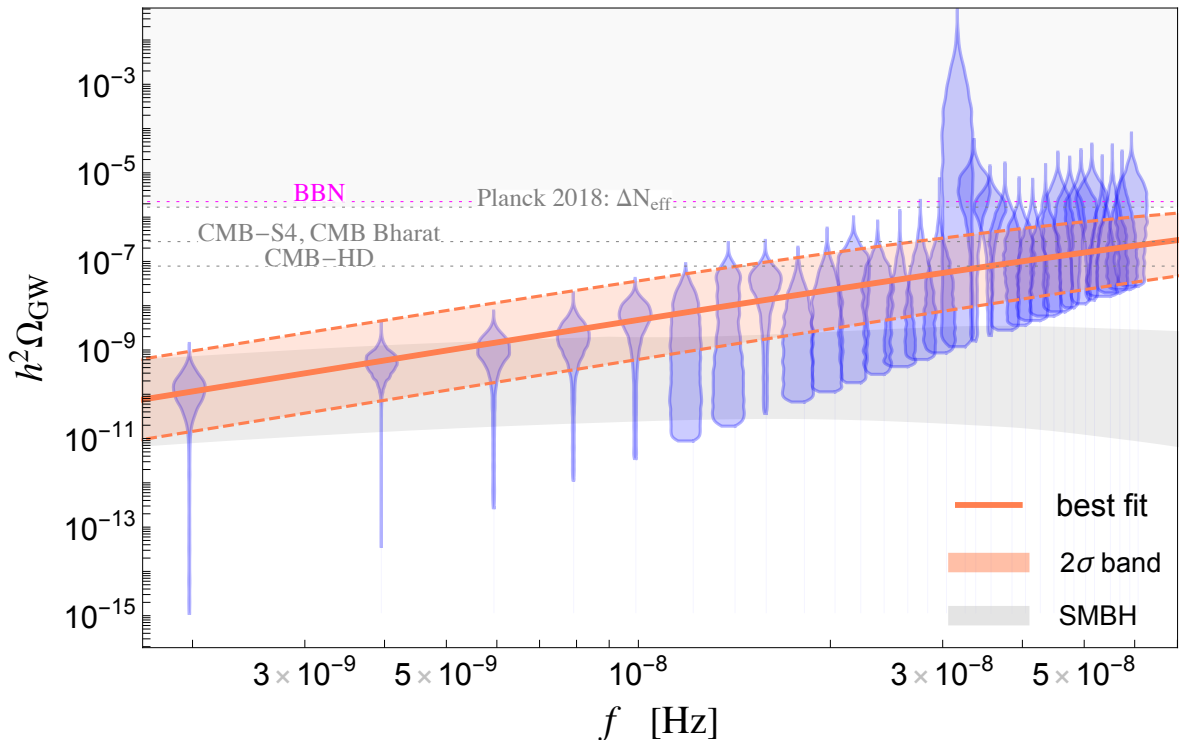


Figure 6. The 15-year data from the NANOGrav collaboration (blue violins) and the best-fit GW spectrum (solid orange, with the 2σ band shown by the orange shaded region) from the supercooled FOPT in our ALP model. For comparison, the expected astrophysical contribution from SMBH is shown by the gray band. Other labels are the same as in Fig. 5.

microlensing-related constraints from HSC (Hyper-Supreme Camera) [241], EROS [242] and Icarus [243], as well as the hint of PBH from OGLE [244] are also shown. We also show the future micro-lensing sensitivity reach of Nancy Grace Roman Space Telescope (NGRST) [245]. Constraints coming from modification of the CMB spectrum due to PBH accretion are shown on the right [246] (see also Ref. [247]). Finally the mass range around M_\odot is constrained by LIGO-VIRGO observations on PBH-PBH merger [119–121, 248–251], while future GW interferometers like ET will be able to set better limits on the PBH abundance [252–257] as depicted by the dashed gray curve in the plot.

Due to the one-to-one correspondence between the PBH mass and the ALP decay constant, we also show in Fig. 7 the f_a values on the upper x -axis. This brings in additional constraints. For instance, the region on the right with $f_a \lesssim 100$ MeV, which roughly corresponds to $T_{\text{RH}} \lesssim 10$ MeV, is excluded by general BBN considerations. Similarly, if the ALP couples to SM photons, electrons or nucleons, stringent laboratory constraints apply on the corresponding couplings $g_{a\gamma\gamma}$, g_{ae} and g_{ann} , respectively (see Section 6). Since these couplings scale as f_a^{-1} (with $\mathcal{O}(1)$ coefficients), upper limits on these couplings can be translated into lower limits on the f_a scale, or upper limits on the PBH mass, as shown by the vertical lines.

Given the PBH constraints in Fig. 7, we take five benchmark points A, B, C, D, E in the allowed region, with the masses of the PBHs formed during the supercooling as $10^{-17.5} M_\odot$,

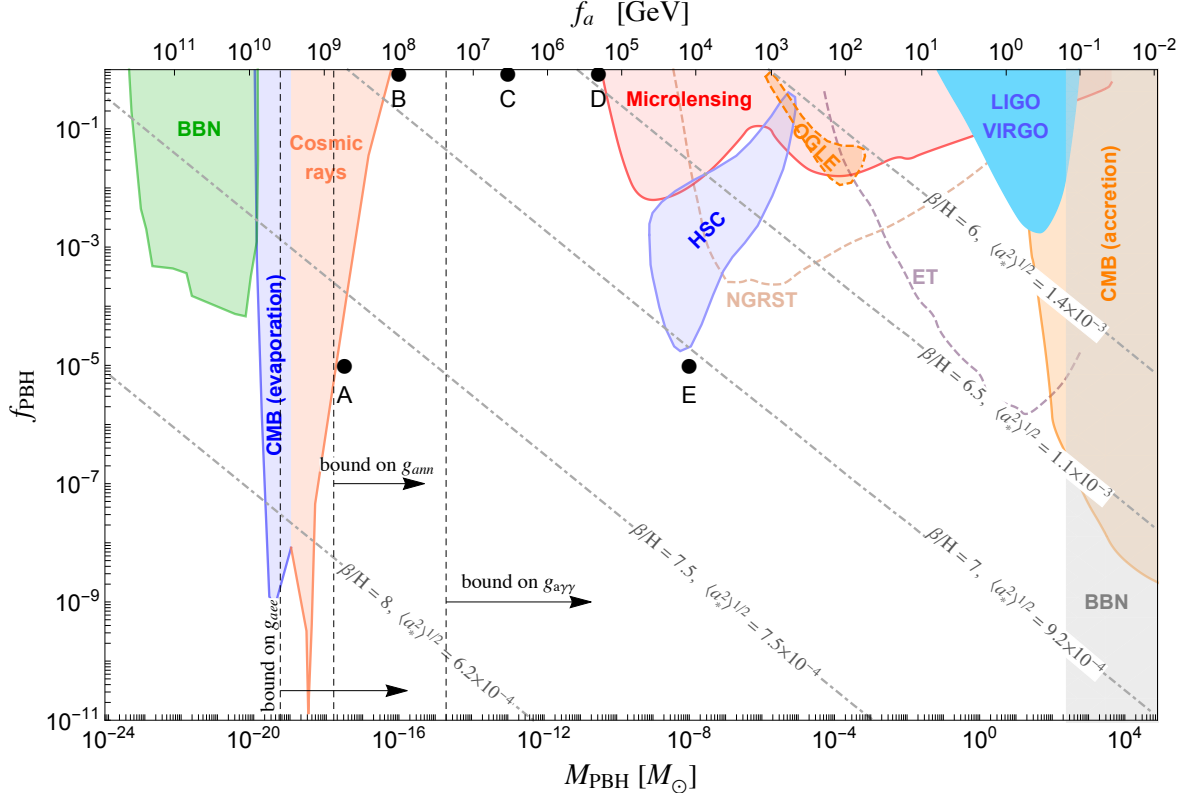


Figure 7. Summary of the PBH constraints. The colored shaded areas are excluded by BBN, CMB, cosmic rays, microlensing and GW observations, as discussed in the text. The future sensitivities of NGRST and ET are shown by the dashed curves. We also depict the initial PBH spin a_* that is formed. The ALP decay constant value corresponding to each PBH mass is shown on the upper x -axis. We also show the stringent experimental constraints from complementary ALP searches (vertical lines) if ALP couples to photons, electrons or nucleons (see Section 6). The gray shaded region on the right edge with $f_a \lesssim 100$ MeV is also excluded by BBN.

$10^{-16}M_\odot$, $10^{-13}M_\odot$, $10^{-10.5}M_\odot$ and $10^{-8}M_\odot$ respectively. While B, C and D correspond to the PBH accounting for the entire DM content of the Universe, for benchmark points A and E, PBHs only comprise 10^{-5} of the DM relic density of the Universe. The GW spectra for these benchmark points are shown in Fig. 5.

The contours of the initial PBH spin a_* that is formed during supercooling [cf. Eq. (4.5)] is also shown in Fig. 7, along with the corresponding β/H values. It is clear that the spin is very small, although nonzero. It is unlikely that such a tiny spin can be observed (e.g. via superradiance).

The five benchmark points chosen in Fig. 7 correspond to PBHs of different masses and abundances. Points B, C, D are with $f_{\text{PBH}} = 1$, whereas A and E are with $f_{\text{PBH}} = 10^{-5}$. Moreover, they all correspond to different initial spin. Also, as shown in Fig. 5, different GW experiments at different frequencies are sensitive to these benchmarks.

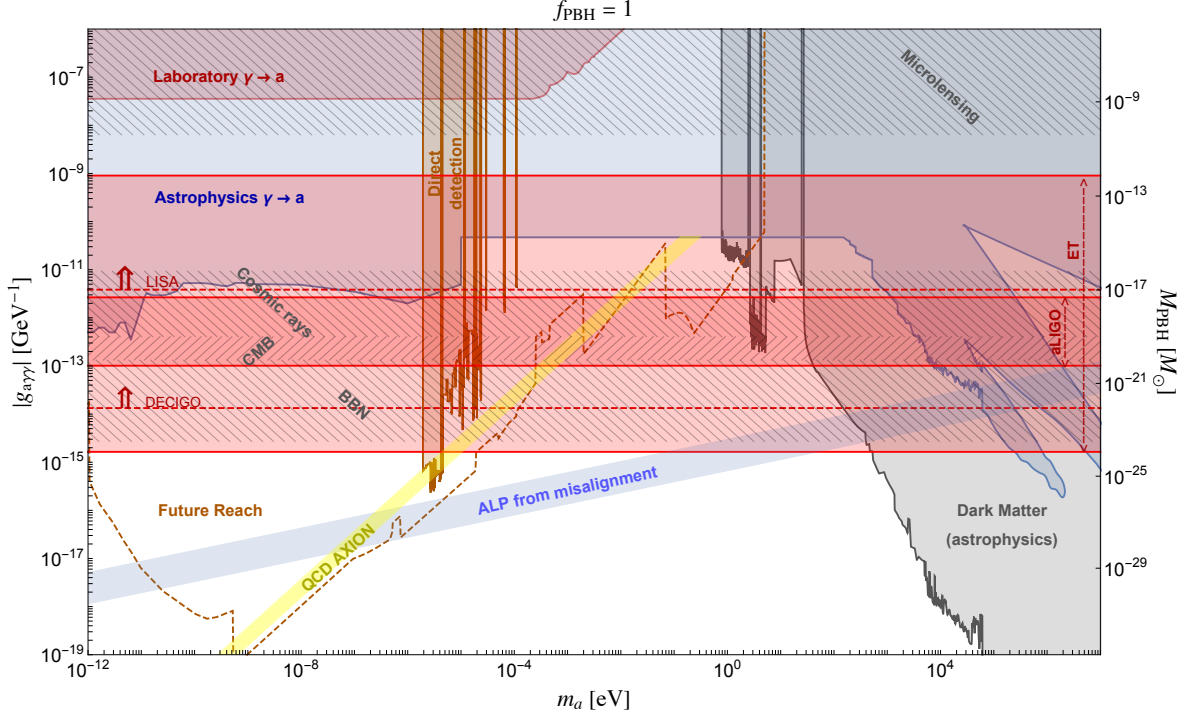


Figure 8. Complementarity between PBH observations, the future GW sensitivities, and constraints on ALP-photon coupling $g_{a\gamma\gamma}$ from laboratory, astrophysical and cosmological constraints. The GW prospects are shown by the red dotted lines. The PBH constraints are shown by the hatched regions. Other available ALP constraints are shown by the shaded regions. See text for more details.

6 Complementarity with laboratory and astrophysical ALP searches

At low energies, the ALP couplings to the SM particles can be induced by higher-dimensional operators. The lowest-order dimension-5 couplings are proportional to the inverse power of f_a . At this order, the effective couplings of the ALP a to the SM photon and fermions can be written as

$$\mathcal{L}_a \supset -\frac{g_{a\gamma\gamma}}{4} a F_{\mu\nu} \tilde{F}^{\mu\nu} - a \sum_f g_{aff} (i\bar{f}\gamma^5 f), \quad (6.1)$$

where $g_{a\gamma\gamma} \simeq \alpha_{\text{em}}/(2\pi f_a)$ and $g_{aff} \simeq m_f/f_a$, neglecting $\mathcal{O}(1)$ coefficients. From Figs. 3 and 5, we see that the GW experiments constrain the scale f_a independently of the ALP mass. Therefore, the GW limits can be translated to limits on the couplings $g_{a\gamma\gamma}$, g_{aee} and g_{ann} for photons, electrons and nucleons respectively [69], which are typically used for laboratory and astrophysical searches of ALPs [167]. Moreover, since f_a is directly correlated with the PBH mass in our ALP model, the constraints on M_{PBH} from Fig. 7 can be translated into constraints on f_a , which in turn can be translated into constraints on the couplings $g_{a\gamma\gamma}$, g_{aee} and g_{ann} . Thus, we get the three-prong complementarity between GW experiments, PBH fraction and ALP searches. This is depicted in Figs. 8, 9 and 10 for $g_{a\gamma\gamma}$, g_{aee} and g_{ann} , respectively with the choice $f_{\text{PBH}} = 1$. Analogous plots with $f_{\text{PBH}} = 10^{-5}$ are given in Appendix A.

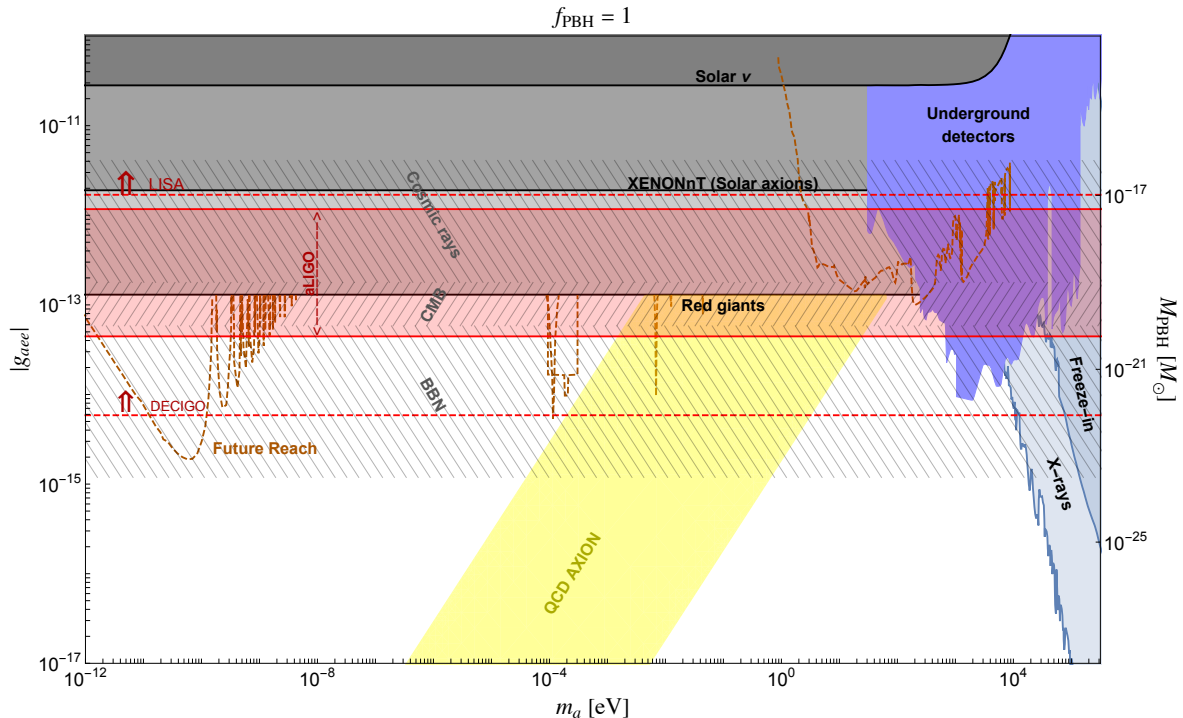


Figure 9. Similar to Fig. 8 but for the ALP coupling to electrons (g_{aee}).

In Fig. 8, different shaded regions correspond to the laboratory constraints (dark red) from light-shining-through-wall (e.g., ALPS [258], CROWS [259], OSQAR [260]), helioscope (e.g., CAST [261]), and haloscope (e.g., ADMX [262]) experiments, as well as astrophysical (blue) constraints from SN1987A [263–265], globular clusters [266], and pulsar polar cap [267] on the ALP-photon coupling. Assuming ALP to be the DM, further astrophysical/cosmological constraints are obtained from late-time ALP decays to photons (from EBL, X-rays, γ -rays, etc) [268, 269] as shown by the bottom-right gray-shaded region. For details, see Refs. [72, 167]. The blue band at the bottom corresponds to the region where ALPs can reproduce the correct DM relic density from the misalignment mechanism [270, 271]. This is especially relevant when the PBH by itself cannot explain all the DM fraction, and the ALP can serve as the remaining DM component. The yellow band is where the QCD axion lives (since $m_a f_a \approx m_\pi f_\pi$) [272]. The dashed curve extending to the bottom shows the projected experimental reach from a combination of future helioscopes, haloscopes and other laboratory experiments [167].

The GW prospects for $g_{a\gamma\gamma}$ are shown by the red dotted lines for future detectors like advanced-LIGO, ET, LISA and DECIGO. We see that the absence of a SGWB at these experiments can constrain additional ALP parameter space beyond the existing limits. More importantly, the *current* constraints on M_{PBH} from BBN, CMB, cosmic rays and microlensing [cf. Fig. 7] are shown here by the hatched regions, some of which turn out to be the most stringent constraints in this parameter space. This is what we call ‘slaying ALPs with PBHs’. Of course, the PBH constraints become weaker if we take $f_{\text{PBH}} < 1$ (see Appendix A).

Similarly, Fig. 9 shows the constraints for the ALP-electron coupling. Here the laboratory constraints include those from underground detectors (blue shaded) such as XENON1T [273,

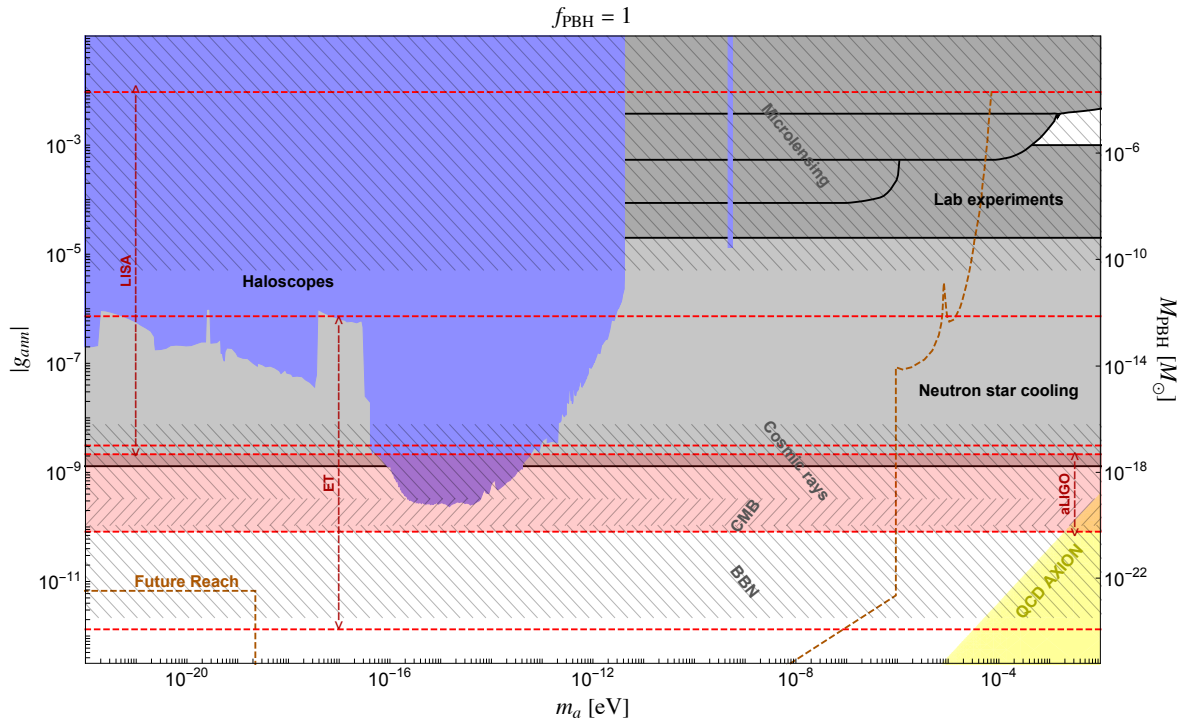


Figure 10. Similar to Fig. 8 but for the ALP coupling to nucleons (g_{ann}).

[274], XENONnT [275], PandaX [276], DarkSide [277], EDELWEISS [278], SuperCDMS [279], and GERDA [280]. The astrophysical constraints (gray/light-blue shaded) include those from solar neutrinos [281], red giant branch [282], X-rays from ALP DM decays [283] and freeze-in [284]. The future projections include novel experiments with NV centers [285] and magnons [286–288]. We again find that the current PBH constraints are actually already ruling out most of the parameter space that could be probed by future laboratory searches, highlighting the usefulness of the complementarity approach discussed here.

Finally, in Fig. 10 we show the constraints on the ALP-nucleon coupling. In this case, the existing haloscope constraints (blue shaded), coming from experiments like CASPER [289], K - ^3He comagnetometer [290], nEDM [291], NASDUCK [292, 293], JEDI [294] and ChangE [295, 296], and astrophysical constraints from isolated neutron star cooling [297] are relevant. But the PBH constraints from BBN and CMB turn out to be the strongest, even cutting into the future laboratory sensitivities.

7 Discussion and Conclusion

In summary, we investigated the GW signal and the formation of PBHs during strong FOPT in an approximately-conformal ALP model. This model already contains a cosmologically stable DM candidate in the form of the ALP, which is basically the phase of the scalar which breaks the $U(1)$ global symmetry via the misalignment mechanism. However, the main point of this work is that a strong FOPT is automatically realized in this scenario due to supercooling from radiative symmetry breaking of the close-to-conformal scalar potential, which not only gives potentially observable stochastic GW signals in future GW experiments,

but also leads to the formation of PBHs that could account for a fraction (or whole) of the DM relic density.

Furthermore, in our model there is a one-to-one correspondence between the ALP decay constant f_a and the PBH mass M_{PBH} . This leads to a three-prong complementarity between the GW signal, PBH signals and other laboratory/astrophysical ALP probes. In particular, depending on the ALP couplings to the SM particles, the ALP constraints can be translated into a lower bound on the PBH mass, independent of f_{PBH} (see Fig. 7). Analogously, we can use the existing PBH constraints to ‘slay’ additional ALP parameter space, which for $f_{\text{PBH}} = 1$ turn out to be even more stringent than the future laboratory searches (see Figs. 8, 9 and 10). This $f_{\text{PBH}} = 1$ region can be tested via the GW signal in future GW detectors like LISA, ET and CE (see Fig. 4). We also discussed the recent NANOGrav detection of a SGWB and its possible interpretation in terms of the FOPT in our ALP scenario (see Fig. 6); however, we find that the NANOGrav-preferred region leads to PBH overclosure.

Note that models of slow roll inflation producing PBHs also result in detectable GWs, in the same frequency range as from the FOPT, due to the enhanced power spectrum on small scales leading to significant anisotropic stress [298–303] or with multiple fields beyond slow roll [129]. However, the GW spectral shapes arising in those scenarios involving second-order tensor perturbations (also known as scalar-induced GW) are quite different from those of PTs, and this could be easily utilized to distinguish between different PBH formation mechanisms.

In future it would be interesting to consider a detailed inflationary scenario which involves modification to the power spectrum on small scales due to the PT, especially in the critical Hubble patches, that would also induce anisotropic stress and a further GW source at second-order, and to study the GW spectral shape features in totality. Due to presence of spectator fields during inflation which undergo PT it may be natural to expect the GW signals observed to be non-Gaussian and to carry features of the primordial spectrum [304]. Also, it would be interesting to go beyond the expected PBH spectrum (beyond the monochromatic approximation used here) from the bubble collision, together with any additional GWs at second order in perturbation theory, in light of testing the $f_{\text{PBH}} = 1$ region at upcoming GW interferometer-based experiments.

Acknowledgments

We thank Priyamvada Natarajan and Kai Schmitz for comments on the draft. A.C. thanks the Galileo Galilei Institute for Theoretical Physics for the hospitality and the INFN for partial support during the completion of this work. This work has been partly funded by the European Union – Next Generation EU through the research grant number P2022Z4P4B “SOPHYA - Sustainable Optimised PHYSics Algorithms: fundamental physics to build an advanced society” under the program PRIN 2022 PNRR of the Italian Ministero dell’Università e Ricerca (MUR) and partially supported by ICSC – Centro Nazionale di Ricerca in High Performance Computing, Big Data and Quantum Computing. The work of B.D. was partly supported by the U.S. Department of Energy under grant No. DE-SC 0017987.

A Supplementary plots

In Figs. 11, 12 and 13 we show the results for a smaller $f_{\text{PBH}} = 10^{-5}$. As expected, the PBH constraints become weaker, compared to the GW and other ALP constraints, which remain unchanged from Figs. 8, 9 and 10, respectively.

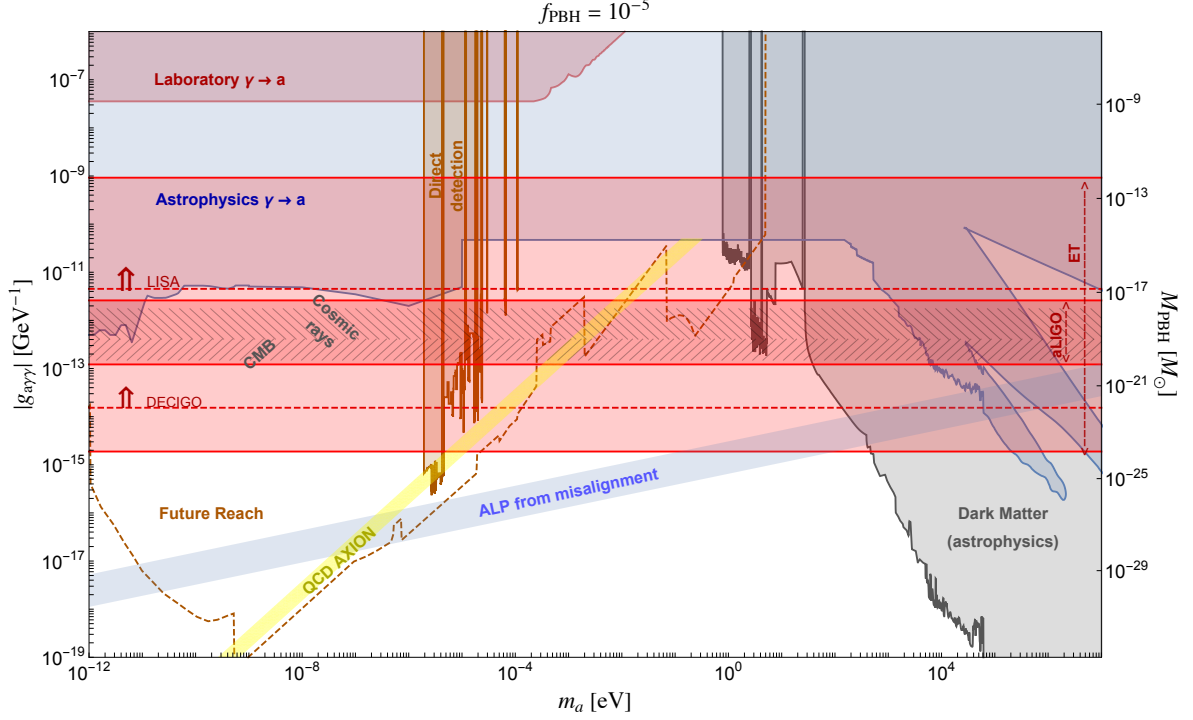


Figure 11. Same as Fig. 8 but for $f_{\text{PBH}} = 10^{-5}$. Only the PBH bounds become weaker, while all other bounds remain the same.

References

- [1] LIGO SCIENTIFIC, VIRGO collaboration, *Observation of Gravitational Waves from a Binary Black Hole Merger*, *Phys. Rev. Lett.* **116** (2016) 061102 [[1602.03837](#)].
- [2] M. Maggiore, *Gravitational wave experiments and early universe cosmology*, *Phys. Rept.* **331** (2000) 283 [[gr-qc/9909001](#)].
- [3] LIGO SCIENTIFIC, VIRGO collaboration, *Upper Limits on the Stochastic Gravitational-Wave Background from Advanced LIGO's First Observing Run*, *Phys. Rev. Lett.* **118** (2017) 121101 [[1612.02029](#)].
- [4] LIGO SCIENTIFIC, VIRGO collaboration, *Search for the isotropic stochastic background using data from Advanced LIGO's second observing run*, *Phys. Rev. D* **100** (2019) 061101 [[1903.02886](#)].
- [5] KAGRA, VIRGO, LIGO SCIENTIFIC collaboration, *Upper limits on the isotropic gravitational-wave background from Advanced LIGO and Advanced Virgo's third observing run*, *Phys. Rev. D* **104** (2021) 022004 [[2101.12130](#)].
- [6] A. Weltman et al., *Fundamental physics with the Square Kilometre Array*, *Publ. Astron. Soc. Austral.* **37** (2020) e002 [[1810.02680](#)].
- [7] J. Garcia-Bellido, H. Murayama and G. White, *Exploring the early Universe with Gaia and Theia*, *JCAP* **12** (2021) 023 [[2104.04778](#)].
- [8] MAGIS-100 collaboration, *Matter-wave Atomic Gradiometer Interferometric Sensor (MAGIS-100)*, *Quantum Sci. Technol.* **6** (2021) 044003 [[2104.02835](#)].

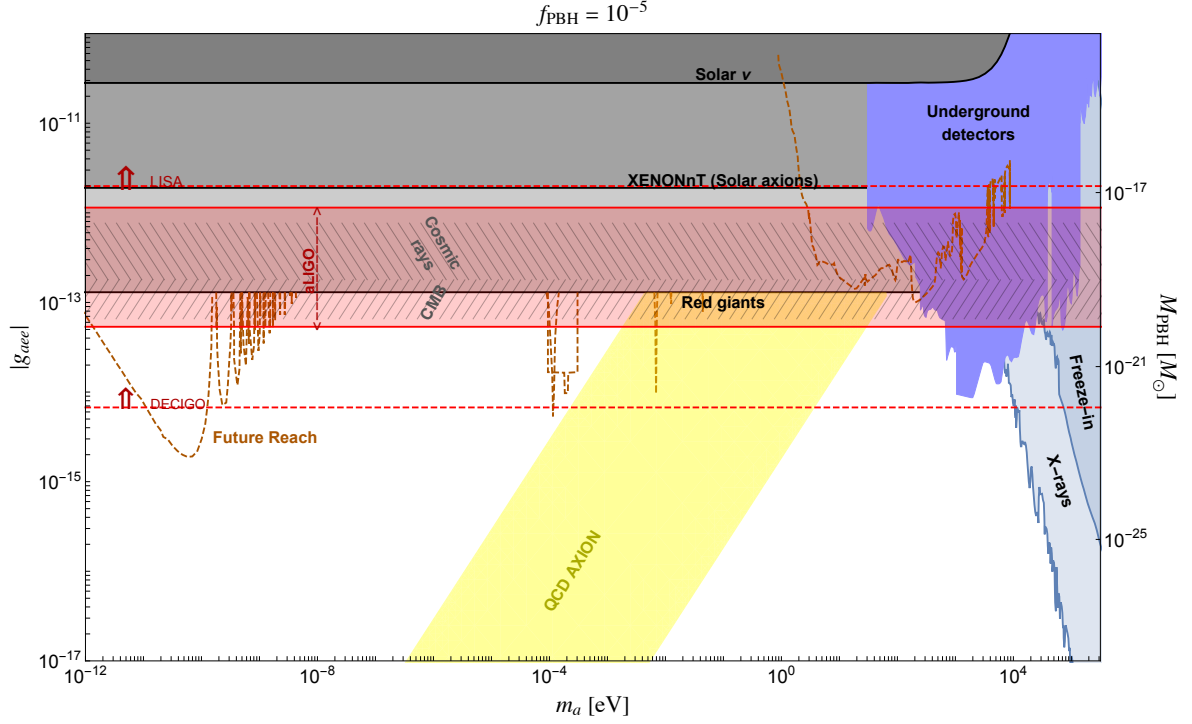


Figure 12. Same as Fig. 9 but for $f_{\text{PBH}} = 10^{-5}$. Only the PBH bounds become weaker, while all other bounds remain the same.

- [9] L. Badurina et al., *AION: An Atom Interferometer Observatory and Network*, *JCAP* **05** (2020) 011 [[1911.11755](#)].
- [10] AEDGE collaboration, *AEDGE: Atomic Experiment for Dark Matter and Gravity Exploration in Space*, *EPJ Quant. Technol.* **7** (2020) 6 [[1908.00802](#)].
- [11] A. Sesana et al., *Unveiling the gravitational universe at μ -Hz frequencies*, *Exper. Astron.* **51** (2021) 1333 [[1908.11391](#)].
- [12] LISA collaboration, *Laser Interferometer Space Antenna*, [1702.00786](#).
- [13] TIANQIN collaboration, *TianQin: a space-borne gravitational wave detector*, *Class. Quant. Grav.* **33** (2016) 035010 [[1512.02076](#)].
- [14] W.-H. Ruan, Z.-K. Guo, R.-G. Cai and Y.-Z. Zhang, *Taiji program: Gravitational-wave sources*, *Int. J. Mod. Phys. A* **35** (2020) 2050075 [[1807.09495](#)].
- [15] S. Kawamura et al., *Current status of space gravitational wave antenna DECIGO and B-DECIGO*, *PTEP* **2021** (2021) 05A105 [[2006.13545](#)].
- [16] V. Corbin and N.J. Cornish, *Detecting the cosmic gravitational wave background with the big bang observer*, *Class. Quant. Grav.* **23** (2006) 2435 [[gr-qc/0512039](#)].
- [17] M. Punturo et al., *The Einstein Telescope: A third-generation gravitational wave observatory*, *Class. Quant. Grav.* **27** (2010) 194002.
- [18] D. Reitze et al., *Cosmic Explorer: The U.S. Contribution to Gravitational-Wave Astronomy beyond LIGO*, *Bull. Am. Astron. Soc.* **51** (2019) 035 [[1907.04833](#)].
- [19] N. Aggarwal et al., *Challenges and opportunities of gravitational-wave searches at MHz to GHz frequencies*, *Living Rev. Rel.* **24** (2021) 4 [[2011.12414](#)].

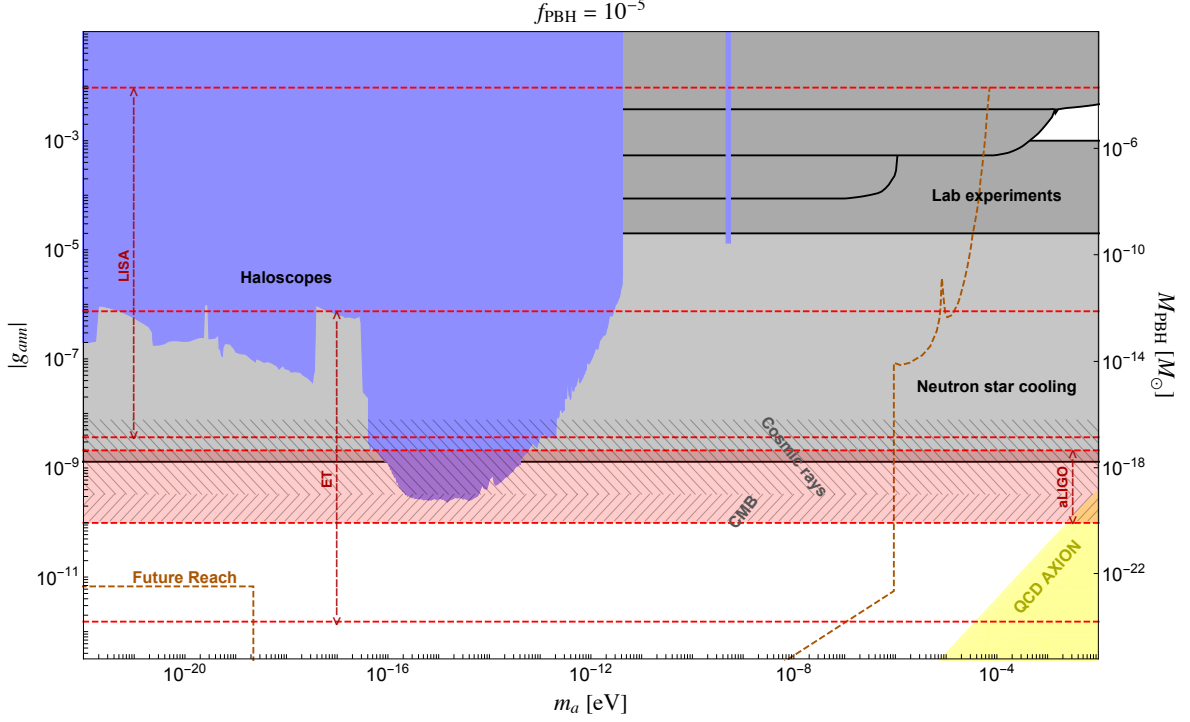


Figure 13. Same as Fig. 10 but for $f_{\text{PBH}} = 10^{-5}$. Only the PBH bounds become weaker, while all other bounds remain the same.

- [20] A. Berlin, D. Blas, R. Tito D’Agnolo, S.A.R. Ellis, R. Harnik, Y. Kahn et al., *Detecting high-frequency gravitational waves with microwave cavities*, *Phys. Rev. D* **105** (2022) 116011 [2112.11465].
- [21] N. Herman, L. Lehoucq and A. F uzfa, *Electromagnetic antennas for the resonant detection of the stochastic gravitational wave background*, *Phys. Rev. D* **108** (2023) 124009 [2203.15668].
- [22] T. Bringmann, V. Domcke, E. Fuchs and J. Kopp, *High-frequency gravitational wave detection via optical frequency modulation*, *Phys. Rev. D* **108** (2023) L061303 [2304.10579].
- [23] NANOGrav collaboration, *The NANOGrav 15 yr Data Set: Evidence for a Gravitational-wave Background*, *Astrophys. J. Lett.* **951** (2023) L8 [2306.16213].
- [24] EPTA, INPTA: collaboration, *The second data release from the European Pulsar Timing Array - III. Search for gravitational wave signals*, *Astron. Astrophys.* **678** (2023) A50 [2306.16214].
- [25] D.J. Reardon et al., *Search for an Isotropic Gravitational-wave Background with the Parkes Pulsar Timing Array*, *Astrophys. J. Lett.* **951** (2023) L6 [2306.16215].
- [26] H. Xu et al., *Searching for the Nano-Hertz Stochastic Gravitational Wave Background with the Chinese Pulsar Timing Array Data Release I*, *Res. Astron. Astrophys.* **23** (2023) 075024 [2306.16216].
- [27] NANOGrav collaboration, *The NANOGrav 15 yr Data Set: Constraints on Supermassive Black Hole Binaries from the Gravitational-wave Background*, *Astrophys. J. Lett.* **952** (2023) L37 [2306.16220].
- [28] NANOGrav collaboration, *The NANOGrav 15 yr Data Set: Search for Signals from New Physics*, *Astrophys. J. Lett.* **951** (2023) L11 [2306.16219].

- [29] EPTA collaboration, *The second data release from the European Pulsar Timing Array: V. Implications for massive black holes, dark matter and the early Universe*, [2306.16227](#).
- [30] R. Roshan and G. White, *Using gravitational waves to see the first second of the Universe*, [2401.04388](#).
- [31] C. Caprini et al., *Science with the space-based interferometer eLISA. II: Gravitational waves from cosmological phase transitions*, *JCAP* **04** (2016) 001 [[1512.06239](#)].
- [32] K. Kajantie, M. Laine, K. Rummukainen and M.E. Shaposhnikov, *Is there a hot electroweak phase transition at $m_H \gtrsim m_W$?*, *Phys. Rev. Lett.* **77** (1996) 2887 [[hep-ph/9605288](#)].
- [33] T. Bhattacharya et al., *QCD Phase Transition with Chiral Quarks and Physical Quark Masses*, *Phys. Rev. Lett.* **113** (2014) 082001 [[1402.5175](#)].
- [34] C. Grojean and G. Servant, *Gravitational Waves from Phase Transitions at the Electroweak Scale and Beyond*, *Phys. Rev. D* **75** (2007) 043507 [[hep-ph/0607107](#)].
- [35] LIGO SCIENTIFIC collaboration, *Advanced LIGO*, *Class. Quant. Grav.* **32** (2015) 074001 [[1411.4547](#)].
- [36] VIRGO collaboration, *Advanced Virgo: a second-generation interferometric gravitational wave detector*, *Class. Quant. Grav.* **32** (2015) 024001 [[1408.3978](#)].
- [37] P.S.B. Dev and A. Mazumdar, *Probing the Scale of New Physics by Advanced LIGO/VIRGO*, *Phys. Rev. D* **93** (2016) 104001 [[1602.04203](#)].
- [38] R.D. Peccei and H.R. Quinn, *CP Conservation in the Presence of Instantons*, *Phys. Rev. Lett.* **38** (1977) 1440.
- [39] R.D. Peccei and H.R. Quinn, *Constraints Imposed by CP Conservation in the Presence of Instantons*, *Phys. Rev. D* **16** (1977) 1791.
- [40] S. Weinberg, *A New Light Boson?*, *Phys. Rev. Lett.* **40** (1978) 223.
- [41] F. Wilczek, *Problem of Strong P and T Invariance in the Presence of Instantons*, *Phys. Rev. Lett.* **40** (1978) 279.
- [42] J. Preskill, M.B. Wise and F. Wilczek, *Cosmology of the Invisible Axion*, *Phys. Lett. B* **120** (1983) 127.
- [43] L.F. Abbott and P. Sikivie, *A Cosmological Bound on the Invisible Axion*, *Phys. Lett. B* **120** (1983) 133.
- [44] M. Dine and W. Fischler, *The Not So Harmless Axion*, *Phys. Lett. B* **120** (1983) 137.
- [45] P. Svrcek and E. Witten, *Axions In String Theory*, *JHEP* **06** (2006) 051 [[hep-th/0605206](#)].
- [46] A. Arvanitaki, S. Dimopoulos, S. Dubovsky, N. Kaloper and J. March-Russell, *String Axiverse*, *Phys. Rev. D* **81** (2010) 123530 [[0905.4720](#)].
- [47] D.J.E. Marsh, *Axion Cosmology*, *Phys. Rept.* **643** (2016) 1 [[1510.07633](#)].
- [48] K. Freese, J.A. Frieman and A.V. Olinto, *Natural inflation with pseudo - Nambu-Goldstone bosons*, *Phys. Rev. Lett.* **65** (1990) 3233.
- [49] F.C. Adams, J.R. Bond, K. Freese, J.A. Frieman and A.V. Olinto, *Natural inflation: Particle physics models, power law spectra for large scale structure, and constraints from COBE*, *Phys. Rev. D* **47** (1993) 426 [[hep-ph/9207245](#)].
- [50] R. Daido, F. Takahashi and W. Yin, *The ALP miracle: unified inflaton and dark matter*, *JCAP* **05** (2017) 044 [[1702.03284](#)].
- [51] R. Daido, N. Kitajima and F. Takahashi, *Axion domain wall baryogenesis*, *JCAP* **07** (2015) 046 [[1504.07917](#)].

- [52] A. De Simone, T. Kobayashi and S. Liberati, *Geometric Baryogenesis from Shift Symmetry*, *Phys. Rev. Lett.* **118** (2017) 131101 [[1612.04824](#)].
- [53] R.T. Co and K. Harigaya, *Axiogenesis*, *Phys. Rev. Lett.* **124** (2020) 111602 [[1910.02080](#)].
- [54] K.S. Jeong, T.H. Jung and C.S. Shin, *Adiabatic electroweak baryogenesis driven by an axionlike particle*, *Phys. Rev. D* **101** (2020) 035009 [[1811.03294](#)].
- [55] S.H. Im, K.S. Jeong and Y. Lee, *Electroweak baryogenesis by axionlike dark matter*, *Phys. Rev. D* **105** (2022) 035028 [[2111.01327](#)].
- [56] J.W. Foster, S. Kumar, B.R. Safdi and Y. Soreq, *Dark Grand Unification in the axiverse: decaying axion dark matter and spontaneous baryogenesis*, *JHEP* **12** (2022) 119 [[2208.10504](#)].
- [57] P. Jain, *Dark energy in an axion model with explicit $Z(N)$ symmetry breaking*, *Mod. Phys. Lett. A* **20** (2005) 1763 [[hep-ph/0411279](#)].
- [58] J.E. Kim and H.P. Nilles, *Axionic dark energy and a composite QCD axion*, *JCAP* **05** (2009) 010 [[0902.3610](#)].
- [59] J.E. Kim and H.P. Nilles, *Dark energy from approximate $U(1)_{de}$ symmetry*, *Phys. Lett. B* **730** (2014) 53 [[1311.0012](#)].
- [60] G. Choi, M. Suzuki and T.T. Yanagida, *Quintessence axion dark energy and a solution to the hubble tension*, *Phys. Lett. B* **805** (2020) 135408 [[1910.00459](#)].
- [61] R. Brandenberger and J. Fröhlich, *Dark Energy, Dark Matter and Baryogenesis from a Model of a Complex Axion Field*, *JCAP* **04** (2021) 030 [[2004.10025](#)].
- [62] Y.-H. Yao and X.-H. Meng, *Restoring cosmological concordance with axion-like early dark energy and dark matter characterized by a constant equation of state?*, [2312.04007](#).
- [63] P.W. Graham, D.E. Kaplan and S. Rajendran, *Cosmological Relaxation of the Electroweak Scale*, *Phys. Rev. Lett.* **115** (2015) 221801 [[1504.07551](#)].
- [64] A. Salvio, *A Simple Motivated Completion of the Standard Model below the Planck Scale: Axions and Right-Handed Neutrinos*, *Phys. Lett. B* **743** (2015) 428 [[1501.03781](#)].
- [65] G. Ballesteros, J. Redondo, A. Ringwald and C. Tamarit, *Standard Model—axion—seesaw—Higgs portal inflation. Five problems of particle physics and cosmology solved in one stroke*, *JCAP* **08** (2017) 001 [[1610.01639](#)].
- [66] Y. Ema, K. Hamaguchi, T. Moroi and K. Nakayama, *Flaxion: a minimal extension to solve puzzles in the standard model*, *JHEP* **01** (2017) 096 [[1612.05492](#)].
- [67] R.S. Gupta, J.Y. Reiness and M. Spannowsky, *All-in-one relaxion: A unified solution to five particle-physics puzzles*, *Phys. Rev. D* **100** (2019) 055003 [[1902.08633](#)].
- [68] A.H. Sopov and R.R. Volkas, *VISH ν : solving five Standard Model shortcomings with a Poincaré-protected electroweak scale*, *Phys. Dark Univ.* **42** (2023) 101381 [[2206.11598](#)].
- [69] P.S.B. Dev, F. Ferrer, Y. Zhang and Y. Zhang, *Gravitational Waves from First-Order Phase Transition in a Simple Axion-Like Particle Model*, *JCAP* **11** (2019) 006 [[1905.00891](#)].
- [70] L. Delle Rose, G. Panico, M. Redi and A. Tesi, *Gravitational Waves from Supercool Axions*, *JHEP* **04** (2020) 025 [[1912.06139](#)].
- [71] B. Von Harling, A. Pomarol, O. Pujolàs and F. Rompineve, *Peccei-Quinn Phase Transition at LIGO*, *JHEP* **04** (2020) 195 [[1912.07587](#)].
- [72] K. Choi, S.H. Im and C. Sub Shin, *Recent Progress in the Physics of Axions and Axion-Like Particles*, *Ann. Rev. Nucl. Part. Sci.* **71** (2021) 225 [[2012.05029](#)].
- [73] J.E. Kim, *Weak Interaction Singlet and Strong CP Invariance*, *Phys. Rev. Lett.* **43** (1979) 103.

- [74] M.A. Shifman, A.I. Vainshtein and V.I. Zakharov, *Can Confinement Ensure Natural CP Invariance of Strong Interactions?*, *Nucl. Phys. B* **166** (1980) 493.
- [75] A.R. Zhitnitsky, *On Possible Suppression of the Axion Hadron Interactions. (In Russian)*, *Sov. J. Nucl. Phys.* **31** (1980) 260.
- [76] M. Dine, W. Fischler and M. Srednicki, *A Simple Solution to the Strong CP Problem with a Harmless Axion*, *Phys. Lett. B* **104** (1981) 199.
- [77] V. Cardoso, O.J.C. Dias, G.S. Hartnett, M. Middleton, P. Pani and J.E. Santos, *Constraining the mass of dark photons and axion-like particles through black-hole superradiance*, *JCAP* **03** (2018) 043 [[1801.01420](#)].
- [78] K.A. Meissner and H. Nicolai, *Conformal Symmetry and the Standard Model*, *Phys. Lett. B* **648** (2007) 312 [[hep-th/0612165](#)].
- [79] S.R. Coleman and E.J. Weinberg, *Radiative Corrections as the Origin of Spontaneous Symmetry Breaking*, *Phys. Rev. D* **7** (1973) 1888.
- [80] E. Witten, *Cosmological Consequences of a Light Higgs Boson*, *Nucl. Phys. B* **177** (1981) 477.
- [81] A. Ghoshal and A. Salvio, *Gravitational waves from fundamental axion dynamics*, *JHEP* **12** (2020) 049 [[2007.00005](#)].
- [82] J. Jaeckel, V.V. Khoze and M. Spannowsky, *Hearing the signal of dark sectors with gravitational wave detectors*, *Phys. Rev. D* **94** (2016) 103519 [[1602.03901](#)].
- [83] R. Jinno and M. Takimoto, *Probing a classically conformal B-L model with gravitational waves*, *Phys. Rev. D* **95** (2017) 015020 [[1604.05035](#)].
- [84] L. Marzola, A. Racioppi and V. Vaskonen, *Phase transition and gravitational wave phenomenology of scalar conformal extensions of the Standard Model*, *Eur. Phys. J. C* **77** (2017) 484 [[1704.01034](#)].
- [85] S. Iso, P.D. Serpico and K. Shimada, *QCD-Electroweak First-Order Phase Transition in a Supercooled Universe*, *Phys. Rev. Lett.* **119** (2017) 141301 [[1704.04955](#)].
- [86] W. Chao, W.-F. Cui, H.-K. Guo and J. Shu, *Gravitational wave imprint of new symmetry breaking*, *Chin. Phys. C* **44** (2020) 123102 [[1707.09759](#)].
- [87] I. Baldes and C. Garcia-Cely, *Strong gravitational radiation from a simple dark matter model*, *JHEP* **05** (2019) 190 [[1809.01198](#)].
- [88] T. Prokopec, J. Rezaeck and B. Świeżewska, *Gravitational waves from conformal symmetry breaking*, *JCAP* **02** (2019) 009 [[1809.11129](#)].
- [89] V. Brdar, A.J. Helmboldt and J. Kubo, *Gravitational Waves from First-Order Phase Transitions: LIGO as a Window to Unexplored Seesaw Scales*, *JCAP* **02** (2019) 021 [[1810.12306](#)].
- [90] C. Marzo, L. Marzola and V. Vaskonen, *Phase transition and vacuum stability in the classically conformal B-L model*, *Eur. Phys. J. C* **79** (2019) 601 [[1811.11169](#)].
- [91] T. Hasegawa, N. Okada and O. Seto, *Gravitational waves from the minimal gauged $U(1)_{B-L}$ model*, *Phys. Rev. D* **99** (2019) 095039 [[1904.03020](#)].
- [92] J. Ellis, M. Lewicki and V. Vaskonen, *Updated predictions for gravitational waves produced in a strongly supercooled phase transition*, *JCAP* **11** (2020) 020 [[2007.15586](#)].
- [93] A. Chikkaballi, K. Kowalska and E.M. Sessolo, *Naturally small neutrino mass with asymptotic safety and gravitational-wave signatures*, *JHEP* **11** (2023) 224 [[2308.06114](#)].
- [94] A. Ahriche, S. Kanemura and M. Tanaka, *Gravitational Waves from Phase Transitions in Scale Invariant Models*, [2308.12676](#).

- [95] P. Huang and K.-P. Xie, *Leptogenesis triggered by a first-order phase transition*, *JHEP* **09** (2022) 052 [[2206.04691](#)].
- [96] A. Dasgupta, P.S.B. Dev, A. Ghoshal and A. Mazumdar, *Gravitational wave pathway to testable leptogenesis*, *Phys. Rev. D* **106** (2022) 075027 [[2206.07032](#)].
- [97] D. Borah, A. Dasgupta and I. Saha, *Leptogenesis and dark matter through relativistic bubble walls with observable gravitational waves*, *JHEP* **11** (2022) 136 [[2207.14226](#)].
- [98] A. Dasgupta, P.S.B. Dev, T. Han, R. Padhan, S. Wang and K. Xie, *Searching for heavy leptophilic Z' : from lepton colliders to gravitational waves*, *JHEP* **12** (2023) 011 [[2308.12804](#)].
- [99] A. Ghoshal, D. Mukherjee and M. Rinaldi, *Inflation and primordial gravitational waves in scale-invariant quadratic gravity with Higgs*, *JHEP* **05** (2023) 023 [[2205.06475](#)].
- [100] M.Y. Khlopov, *Primordial Black Holes*, *Res. Astron. Astrophys.* **10** (2010) 495 [[0801.0116](#)].
- [101] B. Carr, K. Kohri, Y. Sendouda and J. Yokoyama, *Constraints on primordial black holes*, *Rept. Prog. Phys.* **84** (2021) 116902 [[2002.12778](#)].
- [102] B.J. Carr and S.W. Hawking, *Black holes in the early Universe*, *Mon. Not. Roy. Astron. Soc.* **168** (1974) 399.
- [103] B. Carr, F. Kuhnel and M. Sandstad, *Primordial Black Holes as Dark Matter*, *Phys. Rev. D* **94** (2016) 083504 [[1607.06077](#)].
- [104] B. Carr and F. Kuhnel, *Primordial Black Holes as Dark Matter: Recent Developments*, *Ann. Rev. Nucl. Part. Sci.* **70** (2020) 355 [[2006.02838](#)].
- [105] A.M. Green and B.J. Kavanagh, *Primordial Black Holes as a dark matter candidate*, *J. Phys. G* **48** (2021) 043001 [[2007.10722](#)].
- [106] S.W. Hawking, *Black hole explosions*, *Nature* **248** (1974) 30.
- [107] S.W. Hawking, *Particle Creation by Black Holes*, *Commun. Math. Phys.* **43** (1975) 199.
- [108] T. Fujita, M. Kawasaki, K. Harigaya and R. Matsuda, *Baryon asymmetry, dark matter, and density perturbation from primordial black holes*, *Phys. Rev. D* **89** (2014) 103501 [[1401.1909](#)].
- [109] R. Allahverdi, J. Dent and J. Osinski, *Nonthermal production of dark matter from primordial black holes*, *Phys. Rev. D* **97** (2018) 055013 [[1711.10511](#)].
- [110] O. Lennon, J. March-Russell, R. Petrossian-Byrne and H. Tillim, *Black Hole Genesis of Dark Matter*, *JCAP* **04** (2018) 009 [[1712.07664](#)].
- [111] D. Hooper, G. Krnjaic and S.D. McDermott, *Dark Radiation and Superheavy Dark Matter from Black Hole Domination*, *JHEP* **08** (2019) 001 [[1905.01301](#)].
- [112] I. Masina, *Dark matter and dark radiation from evaporating primordial black holes*, *Eur. Phys. J. Plus* **135** (2020) 552 [[2004.04740](#)].
- [113] I. Baldes, Q. Decant, D.C. Hooper and L. Lopez-Honorez, *Non-Cold Dark Matter from Primordial Black Hole Evaporation*, *JCAP* **08** (2020) 045 [[2004.14773](#)].
- [114] P. Gondolo, P. Sandick and B. Shams Es Haghi, *Effects of primordial black holes on dark matter models*, *Phys. Rev. D* **102** (2020) 095018 [[2009.02424](#)].
- [115] N. Bernal and O. Zapata, *Dark Matter in the Time of Primordial Black Holes*, *JCAP* **03** (2021) 015 [[2011.12306](#)].
- [116] S. Bird, I. Cholis, J.B. Muñoz, Y. Ali-Haïmoud, M. Kamionkowski, E.D. Kovetz et al., *Did LIGO detect dark matter?*, *Phys. Rev. Lett.* **116** (2016) 201301 [[1603.00464](#)].
- [117] M. Sasaki, T. Suyama, T. Tanaka and S. Yokoyama, *Primordial Black Hole Scenario for the Gravitational-Wave Event GW150914*, *Phys. Rev. Lett.* **117** (2016) 061101 [[1603.08338](#)].

- [118] S. Clesse and J. García-Bellido, *The clustering of massive Primordial Black Holes as Dark Matter: measuring their mass distribution with Advanced LIGO*, *Phys. Dark Univ.* **15** (2017) 142 [1603.05234].
- [119] G. Hütsi, M. Raidal, V. Vaskonen and H. Veermäe, *Two populations of LIGO-Virgo black holes*, *JCAP* **03** (2021) 068 [2012.02786].
- [120] A. Hall, A.D. Gow and C.T. Byrnes, *Bayesian analysis of LIGO-Virgo mergers: Primordial vs. astrophysical black hole populations*, *Phys. Rev. D* **102** (2020) 123524 [2008.13704].
- [121] G. Franciolini, V. Baibhav, V. De Luca, K.K.Y. Ng, K.W.K. Wong, E. Berti et al., *Searching for a subpopulation of primordial black holes in LIGO-Virgo gravitational-wave data*, *Phys. Rev. D* **105** (2022) 083526 [2105.03349].
- [122] J. He, H. Deng, Y.-S. Piao and J. Zhang, *Implications of GWTC-3 on primordial black holes from vacuum bubbles*, **2303.16810**.
- [123] B. Carr and J. Silk, *Primordial Black Holes as Generators of Cosmic Structures*, *Mon. Not. Roy. Astron. Soc.* **478** (2018) 3756 [1801.00672].
- [124] B. Liu and V. Bromm, *Accelerating Early Massive Galaxy Formation with Primordial Black Holes*, *Astrophys. J. Lett.* **937** (2022) L30 [2208.13178].
- [125] G. Hütsi, M. Raidal, J. Urrutia, V. Vaskonen and H. Veermäe, *Did JWST observe imprints of axion miniclusters or primordial black holes?*, *Phys. Rev. D* **107** (2023) 043502 [2211.02651].
- [126] B.J. Carr, *The Primordial black hole mass spectrum*, *Astrophys. J.* **201** (1975) 1.
- [127] P.S. Cole, A.D. Gow, C.T. Byrnes and S.P. Patil, *Primordial black holes from single-field inflation: a fine-tuning audit*, *JCAP* **08** (2023) 031 [2304.01997].
- [128] A. Ghoshal and A. Strumia, *Traversing a kinetic pole during inflation: primordial black holes and gravitational waves*, **2311.16236**.
- [129] C. Chen, A. Ghoshal, Z. Lalak, Y. Luo and A. Naskar, *Growth of curvature perturbations for PBH formation & detectable GWs in non-minimal curvaton scenario revisited*, *JCAP* **08** (2023) 041 [2305.12325].
- [130] H. Deng and A. Vilenkin, *Primordial black hole formation by vacuum bubbles*, *JCAP* **12** (2017) 044 [1710.02865].
- [131] H. Deng, *Primordial black hole formation by vacuum bubbles. Part II*, *JCAP* **09** (2020) 023 [2006.11907].
- [132] A. Kusenko, M. Sasaki, S. Sugiyama, M. Takada, V. Takhistov and E. Vitagliano, *Exploring Primordial Black Holes from the Multiverse with Optical Telescopes*, *Phys. Rev. Lett.* **125** (2020) 181304 [2001.09160].
- [133] D.N. Maeso, L. Marzola, M. Raidal, V. Vaskonen and H. Veermäe, *Primordial black holes from spectator field bubbles*, *JCAP* **02** (2022) 017 [2112.01505].
- [134] S.W. Hawking, I.G. Moss and J.M. Stewart, *Bubble Collisions in the Very Early Universe*, *Phys. Rev. D* **26** (1982) 2681.
- [135] H. Kodama, M. Sasaki and K. Sato, *Abundance of Primordial Holes Produced by Cosmological First Order Phase Transition*, *Prog. Theor. Phys.* **68** (1982) 1979.
- [136] M. Lewicki and V. Vaskonen, *On bubble collisions in strongly supercooled phase transitions*, *Phys. Dark Univ.* **30** (2020) 100672 [1912.00997].
- [137] A. Ashoorioon, A. Rostami and J.T. Firouzjaee, *Examining the end of inflation with primordial black holes mass distribution and gravitational waves*, *Phys. Rev. D* **103** (2021) 123512 [2012.02817].

- [138] K. Kawana and K.-P. Xie, *Primordial black holes from a cosmic phase transition: The collapse of Fermi-balls*, *Phys. Lett. B* **824** (2022) 136791 [2106.00111].
- [139] J. Liu, L. Bian, R.-G. Cai, Z.-K. Guo and S.-J. Wang, *Primordial black hole production during first-order phase transitions*, *Phys. Rev. D* **105** (2022) L021303 [2106.05637].
- [140] T.H. Jung and T. Okui, *Primordial black holes from bubble collisions during a first-order phase transition*, [2110.04271](#).
- [141] K. Hashino, S. Kanemura, T. Takahashi and M. Tanaka, *Probing first-order electroweak phase transition via primordial black holes in the effective field theory*, *Phys. Lett. B* **838** (2023) 137688 [2211.16225].
- [142] P. Huang and K.-P. Xie, *Primordial black holes from an electroweak phase transition*, *Phys. Rev. D* **105** (2022) 115033 [2201.07243].
- [143] K. Kawana, P. Lu and K.-P. Xie, *First-order phase transition and fate of false vacuum remnants*, *JCAP* **10** (2022) 030 [2206.09923].
- [144] K. Kawana, T. Kim and P. Lu, *PBH formation from overdensities in delayed vacuum transitions*, *Phys. Rev. D* **108** (2023) 103531 [2212.14037].
- [145] M. Kierkla, A. Karam and B. Swiezevska, *Conformal model for gravitational waves and dark matter: a status update*, *JHEP* **03** (2023) 007 [2210.07075].
- [146] M. Kierkla, B. Swiezevska, T.V.I. Tenkanen and J. van de Vis, *Gravitational waves from supercooled phase transitions: dimensional transmutation meets dimensional reduction*, [2312.12413](#).
- [147] S.R. Coleman, *The Fate of the False Vacuum. 1. Semiclassical Theory*, *Phys. Rev. D* **15** (1977) 2929.
- [148] C.G. Callan, Jr. and S.R. Coleman, *The Fate of the False Vacuum. 2. First Quantum Corrections*, *Phys. Rev. D* **16** (1977) 1762.
- [149] A.D. Linde, *Decay of the False Vacuum at Finite Temperature*, *Nucl. Phys. B* **216** (1983) 421.
- [150] K. Sato, M. Sasaki, H. Kodama and K.-i. Maeda, *Creation of Wormholes by First Order Phase Transition of a Vacuum in the Early Universe*, *Prog. Theor. Phys.* **65** (1981) 1443.
- [151] H. Kodama, M. Sasaki, K. Sato and K.-i. Maeda, *Fate of Wormholes Created by First Order Phase Transition in the Early Universe*, *Prog. Theor. Phys.* **66** (1981) 2052.
- [152] K.-i. Maeda, K. Sato, M. Sasaki and H. Kodama, *Creation of De Sitter-schwarzschild Wormholes by a Cosmological First Order Phase Transition*, *Phys. Lett. B* **108** (1982) 98.
- [153] K. Sato, H. Kodama, M. Sasaki and K.-i. Maeda, *Multiproduction of Universes by First Order Phase Transition of a Vacuum*, *Phys. Lett. B* **108** (1982) 103.
- [154] S.D.H. Hsu, *Black Holes From Extended Inflation*, *Phys. Lett. B* **251** (1990) 343.
- [155] K. Hashino, S. Kanemura and T. Takahashi, *Primordial black holes as a probe of strongly first-order electroweak phase transition*, *Phys. Lett. B* **833** (2022) 137261 [2111.13099].
- [156] S. He, L. Li, Z. Li and S.-J. Wang, *Gravitational Waves and Primordial Black Hole Productions from Gluodynamics*, [2210.14094](#).
- [157] T.C. Gehrman, B. Shams Es Haghi, K. Sinha and T. Xu, *The primordial black holes that disappeared: connections to dark matter and MHz-GHz gravitational Waves*, *JCAP* **10** (2023) 001 [2304.09194].
- [158] M. Lewicki, P. Toczek and V. Vaskonen, *Primordial black holes from strong first-order phase transitions*, *JHEP* **09** (2023) 092 [2305.04924].
- [159] Y. Gouttenoire and T. Volansky, *Primordial Black Holes from Supercooled Phase Transitions*, [2305.04942](#).

- [160] I. Baldes and M.O. Olea-Romacho, *Primordial black holes as dark matter: Interferometric tests of phase transition origin*, [2307.11639](#).
- [161] A. Salvio, *Supercooling in Radiative Symmetry Breaking: Theory Extensions, Gravitational Wave Detection and Primordial Black Holes*, *JCAP* **12** (2023) 046 [[2307.04694](#)].
- [162] I.K. Banerjee and U.K. Dey, *Spinning Primordial Black Holes from First Order Phase Transition*, [2311.03406](#).
- [163] Y. Gouttenoire, *First-Order Phase Transition Interpretation of Pulsar Timing Array Signal Is Consistent with Solar-Mass Black Holes*, *Phys. Rev. Lett.* **131** (2023) 171404 [[2307.04239](#)].
- [164] S. He, L. Li, S. Wang and S.-J. Wang, *Constraints on holographic QCD phase transitions from PTA observations*, [2308.07257](#).
- [165] J. Ellis, M. Fairbairn, G. Franciolini, G. Hütsi, A. Iovino, M. Lewicki et al., *What is the source of the PTA GW signal?*, [2308.08546](#).
- [166] B.J. Kavanagh, “Pbhbounds.” <https://github.com/bradkav/PBHbounds>, 2020. 10.5281/zenodo.3538999.
- [167] C. O’Hare, “Axionlimits.” <https://cajohare.github.io/AxionLimits/>, 2020. 10.5281/zenodo.3932430.
- [168] E. Gildener and S. Weinberg, *Symmetry Breaking and Scalar Bosons*, *Phys. Rev. D* **13** (1976) 3333.
- [169] A. Salvio, *Model-independent radiative symmetry breaking and gravitational waves*, *JCAP* **04** (2023) 051 [[2302.10212](#)].
- [170] T. Hambye and A. Strumia, *Dynamical generation of the weak and Dark Matter scale*, *Phys. Rev. D* **88** (2013) 055022 [[1306.2329](#)].
- [171] T. Hambye, A. Strumia and D. Teresi, *Super-cool Dark Matter*, *JHEP* **08** (2018) 188 [[1805.01473](#)].
- [172] J. Kearney, H. Yoo and K.M. Zurek, *Is a Higgs Vacuum Instability Fatal for High-Scale Inflation?*, *Phys. Rev. D* **91** (2015) 123537 [[1503.05193](#)].
- [173] A. Joti, A. Katsis, D. Loupas, A. Salvio, A. Strumia, N. Tetradis et al., *(Higgs) vacuum decay during inflation*, *JHEP* **07** (2017) 058 [[1706.00792](#)].
- [174] A. Kosowsky, M.S. Turner and R. Watkins, *Gravitational waves from first order cosmological phase transitions*, *Phys. Rev. Lett.* **69** (1992) 2026.
- [175] M. Lewicki and V. Vaskonen, *Gravitational waves from colliding vacuum bubbles in gauge theories*, *Eur. Phys. J. C* **81** (2021) 437 [[2012.07826](#)].
- [176] M. Lewicki and V. Vaskonen, *Gravitational wave spectra from strongly supercooled phase transitions*, *Eur. Phys. J. C* **80** (2020) 1003 [[2007.04967](#)].
- [177] D. Cutting, E.G. Escartin, M. Hindmarsh and D.J. Weir, *Gravitational waves from vacuum first order phase transitions II: from thin to thick walls*, *Phys. Rev. D* **103** (2021) 023531 [[2005.13537](#)].
- [178] R. Jinno and M. Takimoto, *Gravitational waves from bubble dynamics: Beyond the Envelope*, *JCAP* **01** (2019) 060 [[1707.03111](#)].
- [179] T. Konstandin, *Gravitational radiation from a bulk flow model*, *JCAP* **03** (2018) 047 [[1712.06869](#)].
- [180] R. Durrer and C. Caprini, *Primordial magnetic fields and causality*, *JCAP* **11** (2003) 010 [[astro-ph/0305059](#)].
- [181] C. Caprini, R. Durrer, T. Konstandin and G. Servant, *General Properties of the Gravitational Wave Spectrum from Phase Transitions*, *Phys. Rev. D* **79** (2009) 083519 [[0901.1661](#)].

- [182] G. Barenboim and W.-I. Park, *Gravitational waves from first order phase transitions as a probe of an early matter domination era and its inverse problem*, *Phys. Lett. B* **759** (2016) 430 [1605.03781].
- [183] R.-G. Cai, S. Pi and M. Sasaki, *Universal infrared scaling of gravitational wave background spectra*, *Phys. Rev. D* **102** (2020) 083528 [1909.13728].
- [184] A. Hook, G. Marques-Tavares and D. Racco, *Causal gravitational waves as a probe of free streaming particles and the expansion of the Universe*, *JHEP* **02** (2021) 117 [2010.03568].
- [185] I. Musco, J.C. Miller and L. Rezzolla, *Computations of primordial black hole formation*, *Class. Quant. Grav.* **22** (2005) 1405 [gr-qc/0412063].
- [186] A. Escrivà and A.E. Romano, *Effects of the shape of curvature peaks on the size of primordial black holes*, *JCAP* **05** (2021) 066 [2103.03867].
- [187] J. Liu, L. Bian, R.-G. Cai, Z.-K. Guo and S.-J. Wang, *Constraining First-Order Phase Transitions with Curvature Perturbations*, *Phys. Rev. Lett.* **130** (2023) 051001 [2208.14086].
- [188] S. Jaraba and J. Garcia-Bellido, *Black hole induced spins from hyperbolic encounters in dense clusters*, *Phys. Dark Univ.* **34** (2021) 100882 [2106.01436].
- [189] F. Hofmann, E. Barausse and L. Rezzolla, *The final spin from binary black holes in quasi-circular orbits*, *Astrophys. J. Lett.* **825** (2016) L19 [1605.01938].
- [190] M. Calzà, J. March-Russell and J.a.G. Rosa, *Evaporating primordial black holes, the string axiverse, and hot dark radiation*, **2110.13602**.
- [191] C.-M. Yoo, T. Harada, J. Garriga and K. Kohri, *Primordial black hole abundance from random Gaussian curvature perturbations and a local density threshold*, *PTEP* **2018** (2018) 123E01 [1805.03946].
- [192] V. De Luca, V. Desjacques, G. Franciolini, A. Malhotra and A. Riotto, *The initial spin probability distribution of primordial black holes*, *JCAP* **05** (2019) 018 [1903.01179].
- [193] T. Harada, C.-M. Yoo, K. Kohri, Y. Koga and T. Monobe, *Spins of primordial black holes formed in the radiation-dominated phase of the universe: first-order effect*, *Astrophys. J.* **908** (2021) 140 [2011.00710].
- [194] PLANCK collaboration, *Planck 2018 results. VI. Cosmological parameters*, *Astron. Astrophys.* **641** (2020) A6 [1807.06209].
- [195] CMB-S4 collaboration, *CMB-S4: Forecasting Constraints on Primordial Gravitational Waves*, *Astrophys. J.* **926** (2022) 54 [2008.12619].
- [196] CMB-S4 collaboration, *Snowmass 2021 CMB-S4 White Paper*, **2203.08024**.
- [197] CMB-BHARAT collaboration, *CMB-Bharat*, <http://cmb-bharat.in>.
- [198] N. Sehgal et al., *CMB-HD: An Ultra-Deep, High-Resolution Millimeter-Wave Survey Over Half the Sky*, **1906.10134**.
- [199] CMB-HD collaboration, *Snowmass2021 CMB-HD White Paper*, **2203.05728**.
- [200] LIGO SCIENTIFIC, VIRGO collaboration, *Open data from the first and second observing runs of Advanced LIGO and Advanced Virgo*, *SoftwareX* **13** (2021) 100658 [1912.11716].
- [201] S. Hild et al., *Sensitivity Studies for Third-Generation Gravitational Wave Observatories*, *Class. Quant. Grav.* **28** (2011) 094013 [1012.0908].
- [202] LIGO SCIENTIFIC collaboration, *Exploring the Sensitivity of Next Generation Gravitational Wave Detectors*, *Class. Quant. Grav.* **34** (2017) 044001 [1607.08697].
- [203] J. Baker et al., *The Laser Interferometer Space Antenna: Unveiling the Millihertz Gravitational Wave Sky*, **1907.06482**.

- [204] J. Crowder and N.J. Cornish, *Beyond LISA: Exploring future gravitational wave missions*, *Phys. Rev. D* **72** (2005) 083005 [gr-qc/0506015].
- [205] K. Yagi and N. Seto, *Detector configuration of DECIGO/BBO and identification of cosmological neutron-star binaries*, *Phys. Rev. D* **83** (2011) 044011 [1101.3940].
- [206] L. Badurina, O. Buchmueller, J. Ellis, M. Lewicki, C. McCabe and V. Vaskonen, *Prospective sensitivities of atom interferometers to gravitational waves and ultralight dark matter*, *Phil. Trans. A. Math. Phys. Eng. Sci.* **380** (2021) 20210060 [2108.02468].
- [207] L. Lentati et al., *European Pulsar Timing Array Limits On An Isotropic Stochastic Gravitational-Wave Background*, *Mon. Not. Roy. Astron. Soc.* **453** (2015) 2576 [1504.03692].
- [208] S. Babak et al., *European Pulsar Timing Array Limits on Continuous Gravitational Waves from Individual Supermassive Black Hole Binaries*, *Mon. Not. Roy. Astron. Soc.* **455** (2016) 1665 [1509.02165].
- [209] M. Riajul Haque, E. Kpatcha, D. Maity and Y. Mambrini, *Primordial black hole reheating*, *Phys. Rev. D* **108** (2023) 063523 [2305.10518].
- [210] E. Thrane and J.D. Romano, *Sensitivity curves for searches for gravitational-wave backgrounds*, *Phys. Rev. D* **88** (2013) 124032 [1310.5300].
- [211] LIGO SCIENTIFIC, VIRGO collaboration, *GW150914: Implications for the stochastic gravitational wave background from binary black holes*, *Phys. Rev. Lett.* **116** (2016) 131102 [1602.03847].
- [212] LIGO SCIENTIFIC, VIRGO collaboration, *GWTC-1: A Gravitational-Wave Transient Catalog of Compact Binary Mergers Observed by LIGO and Virgo during the First and Second Observing Runs*, *Phys. Rev. X* **9** (2019) 031040 [1811.12907].
- [213] A.H. Nitz, S. Kumar, Y.-F. Wang, S. Kastha, S. Wu, M. Schäfer et al., *4-OGC: Catalog of Gravitational Waves from Compact Binary Mergers*, *Astrophys. J.* **946** (2023) 59 [2112.06878].
- [214] C. Cutler and J. Harms, *BBO and the neutron-star-binary subtraction problem*, *Phys. Rev. D* **73** (2006) 042001 [gr-qc/0511092].
- [215] X.-J. Zhu, E.J. Howell, D.G. Blair and Z.-H. Zhu, *On the gravitational wave background from compact binary coalescences in the band of ground-based interferometers*, *Mon. Not. Roy. Astron. Soc.* **431** (2013) 882 [1209.0595].
- [216] T. Regimbau, M. Evans, N. Christensen, E. Katsavounidis, B. Sathyaprakash and S. Vitale, *Digging deeper: Observing primordial gravitational waves below the binary black hole produced stochastic background*, *Phys. Rev. Lett.* **118** (2017) 151105 [1611.08943].
- [217] S. Sachdev, T. Regimbau and B.S. Sathyaprakash, *Subtracting compact binary foreground sources to reveal primordial gravitational-wave backgrounds*, *Phys. Rev. D* **102** (2020) 024051 [2002.05365].
- [218] B. Zhou, L. Reali, E. Berti, M. Çalışkan, C. Creque-Sarbinowski, M. Kamionkowski et al., *Subtracting compact binary foregrounds to search for subdominant gravitational-wave backgrounds in next-generation ground-based observatories*, *Phys. Rev. D* **108** (2023) 064040 [2209.01310].
- [219] H. Zhong, R. Ormiston and V. Mandic, *Detecting cosmological gravitational wave background after removal of compact binary coalescences in future gravitational wave detectors*, *Phys. Rev. D* **107** (2023) 064048 [2209.11877].
- [220] Z. Pan and H. Yang, *Improving the detection sensitivity to primordial stochastic gravitational waves with reduced astrophysical foregrounds*, *Phys. Rev. D* **107** (2023) 123036 [2301.04529].

- [221] D.S. Bellie, S. Banagiri, Z. Doctor and V. Kalogera, *The unresolved stochastic background from compact binary mergers detectable by next-generation ground-based gravitational-wave observatories*, [2310.02517](#).
- [222] H. Song, D. Liang, Z. Wang and L. Shao, *Compact Binary Foreground Subtraction for Detecting the Stochastic Gravitational-wave Background in Ground-based Detectors*, [2401.00984](#).
- [223] A.J. Farmer and E.S. Phinney, *The gravitational wave background from cosmological compact binaries*, *Mon. Not. Roy. Astron. Soc.* **346** (2003) 1197 [[astro-ph/0304393](#)].
- [224] P.A. Rosado, *Gravitational wave background from binary systems*, *Phys. Rev. D* **84** (2011) 084004 [[1106.5795](#)].
- [225] C.J. Moore, R.H. Cole and C.P.L. Berry, *Gravitational-wave sensitivity curves*, *Class. Quant. Grav.* **32** (2015) 015014 [[1408.0740](#)].
- [226] D.I. Kosenko and K.A. Postnov, *On the gravitational wave noise from unresolved extragalactic binaries*, *Astron. Astrophys.* **336** (1998) 786 [[astro-ph/9801032](#)].
- [227] M.R. Adams and N.J. Cornish, *Discriminating between a Stochastic Gravitational Wave Background and Instrument Noise*, *Phys. Rev. D* **82** (2010) 022002 [[1002.1291](#)].
- [228] M.R. Adams and N.J. Cornish, *Detecting a Stochastic Gravitational Wave Background in the presence of a Galactic Foreground and Instrument Noise*, *Phys. Rev. D* **89** (2014) 022001 [[1307.4116](#)].
- [229] C. Wu, V. Mandic and T. Regimbau, *Accessibility of the Gravitational-Wave Background due to Binary Coalescences to Second and Third Generation Gravitational-Wave Detectors*, *Phys. Rev. D* **85** (2012) 104024 [[1112.1898](#)].
- [230] P.A. Rosado, A. Sesana and J. Gair, *Expected properties of the first gravitational wave signal detected with pulsar timing arrays*, *Mon. Not. Roy. Astron. Soc.* **451** (2015) 2417 [[1503.04803](#)].
- [231] A.K. Saha and R. Laha, *Sensitivities on nonspinning and spinning primordial black hole dark matter with global 21-cm troughs*, *Phys. Rev. D* **105** (2022) 103026 [[2112.10794](#)].
- [232] R. Laha, *Primordial Black Holes as a Dark Matter Candidate Are Severely Constrained by the Galactic Center 511 keV γ -Ray Line*, *Phys. Rev. Lett.* **123** (2019) 251101 [[1906.09994](#)].
- [233] A. Ray, R. Laha, J.B. Muñoz and R. Caputo, *Near future MeV telescopes can discover asteroid-mass primordial black hole dark matter*, *Phys. Rev. D* **104** (2021) 023516 [[2102.06714](#)].
- [234] S. Clark, B. Dutta, Y. Gao, L.E. Strigari and S. Watson, *Planck Constraint on Relic Primordial Black Holes*, *Phys. Rev. D* **95** (2017) 083006 [[1612.07738](#)].
- [235] S. Mittal, A. Ray, G. Kulkarni and B. Dasgupta, *Constraining primordial black holes as dark matter using the global 21-cm signal with X-ray heating and excess radio background*, *JCAP* **03** (2022) 030 [[2107.02190](#)].
- [236] R. Laha, J.B. Muñoz and T.R. Slatyer, *INTEGRAL constraints on primordial black holes and particle dark matter*, *Phys. Rev. D* **101** (2020) 123514 [[2004.00627](#)].
- [237] J. Berteaud, F. Calore, J. Iguaz, P.D. Serpico and T. Siebert, *Strong constraints on primordial black hole dark matter from 16 years of INTEGRAL/SPI observations*, *Phys. Rev. D* **106** (2022) 023030 [[2202.07483](#)].
- [238] M. Boudaud and M. Cirelli, *Voyager 1 e^\pm Further Constrain Primordial Black Holes as Dark Matter*, *Phys. Rev. Lett.* **122** (2019) 041104 [[1807.03075](#)].
- [239] W. DeRocco and P.W. Graham, *Constraining Primordial Black Hole Abundance with the Galactic 511 keV Line*, *Phys. Rev. Lett.* **123** (2019) 251102 [[1906.07740](#)].

- [240] B.J. Carr, K. Kohri, Y. Sendouda and J. Yokoyama, *New cosmological constraints on primordial black holes*, *Phys. Rev. D* **81** (2010) 104019 [0912.5297].
- [241] H. Niikura et al., *Microlensing constraints on primordial black holes with Subaru/HSC Andromeda observations*, *Nature Astron.* **3** (2019) 524 [1701.02151].
- [242] EROS-2 collaboration, *Limits on the Macho Content of the Galactic Halo from the EROS-2 Survey of the Magellanic Clouds*, *Astron. Astrophys.* **469** (2007) 387 [astro-ph/0607207].
- [243] M. Oguri, J.M. Diego, N. Kaiser, P.L. Kelly and T. Broadhurst, *Understanding caustic crossings in giant arcs: characteristic scales, event rates, and constraints on compact dark matter*, *Phys. Rev. D* **97** (2018) 023518 [1710.00148].
- [244] H. Niikura, M. Takada, S. Yokoyama, T. Sumi and S. Masaki, *Constraints on Earth-mass primordial black holes from OGLE 5-year microlensing events*, *Phys. Rev. D* **99** (2019) 083503 [1901.07120].
- [245] W. DeRocco, E. Frangipane, N. Hamer, S. Profumo and N. Smyth, *Rogue worlds meet the dark side: revealing terrestrial-mass primordial black holes with the Nancy Grace Roman Space Telescope*, **2311.00751**.
- [246] P.D. Serpico, V. Poulin, D. Inman and K. Kohri, *Cosmic microwave background bounds on primordial black holes including dark matter halo accretion*, *Phys. Rev. Res.* **2** (2020) 023204 [2002.10771].
- [247] L. Piga, M. Lucca, N. Bellomo, V. Bosch-Ramon, S. Matarrese, A. Raccanelli et al., *The effect of outflows on CMB bounds from Primordial Black Hole accretion*, *JCAP* **12** (2022) 016 [2210.14934].
- [248] G. Franciolini, I. Musco, P. Pani and A. Urbano, *From inflation to black hole mergers and back again: Gravitational-wave data-driven constraints on inflationary scenarios with a first-principle model of primordial black holes across the QCD epoch*, *Phys. Rev. D* **106** (2022) 123526 [2209.05959].
- [249] B.J. Kavanagh, D. Gaggero and G. Bertone, *Merger rate of a subdominant population of primordial black holes*, *Phys. Rev. D* **98** (2018) 023536 [1805.09034].
- [250] K.W.K. Wong, G. Franciolini, V. De Luca, V. Baibhav, E. Berti, P. Pani et al., *Constraining the primordial black hole scenario with Bayesian inference and machine learning: the GWTC-2 gravitational wave catalog*, *Phys. Rev. D* **103** (2021) 023026 [2011.01865].
- [251] V. De Luca, G. Franciolini, P. Pani and A. Riotto, *Bayesian Evidence for Both Astrophysical and Primordial Black Holes: Mapping the GWTC-2 Catalog to Third-Generation Detectors*, *JCAP* **05** (2021) 003 [2102.03809].
- [252] V. De Luca, G. Franciolini, P. Pani and A. Riotto, *The minimum testable abundance of primordial black holes at future gravitational-wave detectors*, *JCAP* **11** (2021) 039 [2106.13769].
- [253] O. Pujolas, V. Vaskonen and H. Veermäe, *Prospects for probing gravitational waves from primordial black hole binaries*, *Phys. Rev. D* **104** (2021) 083521 [2107.03379].
- [254] G. Franciolini, A. Maharana and F. Muia, *Hunt for light primordial black hole dark matter with ultrahigh-frequency gravitational waves*, *Phys. Rev. D* **106** (2022) 103520 [2205.02153].
- [255] M. Martinelli, F. Scarcella, N.B. Hogg, B.J. Kavanagh, D. Gaggero and P. Fleury, *Dancing in the dark: detecting a population of distant primordial black holes*, *JCAP* **08** (2022) 006 [2205.02639].
- [256] G. Franciolini, F. Iacovelli, M. Mancarella, M. Maggiore, P. Pani and A. Riotto, *Searching for primordial black holes with the Einstein Telescope: Impact of design and systematics*, *Phys. Rev. D* **108** (2023) 043506 [2304.03160].

- [257] M. Branchesi et al., *Science with the Einstein Telescope: a comparison of different designs*, *JCAP* **07** (2023) 068 [2303.15923].
- [258] K. Ehret et al., *New ALPS Results on Hidden-Sector Lightweights*, *Phys. Lett. B* **689** (2010) 149 [1004.1313].
- [259] M. Betz, F. Caspers, M. Gasior, M. Thumm and S.W. Rieger, *First results of the CERN Resonant Weakly Interacting sub-eV Particle Search (CROWS)*, *Phys. Rev. D* **88** (2013) 075014 [1310.8098].
- [260] OSQAR collaboration, *New exclusion limits on scalar and pseudoscalar axionlike particles from light shining through a wall*, *Phys. Rev. D* **92** (2015) 092002 [1506.08082].
- [261] CAST collaboration, *New CAST Limit on the Axion-Photon Interaction*, *Nature Phys.* **13** (2017) 584 [1705.02290].
- [262] ADMX collaboration, *Search for Invisible Axion Dark Matter in the 3.3–4.2 μeV Mass Range*, *Phys. Rev. Lett.* **127** (2021) 261803 [2110.06096].
- [263] A. Caputo, H.-T. Janka, G. Raffelt and E. Vitagliano, *Low-Energy Supernovae Severely Constrain Radiative Particle Decays*, *Phys. Rev. Lett.* **128** (2022) 221103 [2201.09890].
- [264] M. Diamond, D.F.G. Fiorillo, G. Marques-Tavares and E. Vitagliano, *Axion-sourced fireballs from supernovae*, *Phys. Rev. D* **107** (2023) 103029 [2303.11395].
- [265] E. Müller, F. Calore, P. Carena, C. Eckner and M.C.D. Marsh, *Investigating the gamma-ray burst from decaying MeV-scale axion-like particles produced in supernova explosions*, *JCAP* **07** (2023) 056 [2304.01060].
- [266] M.J. Dolan, F.J. Hiskens and R.R. Volkas, *Advancing globular cluster constraints on the axion-photon coupling*, *JCAP* **10** (2022) 096 [2207.03102].
- [267] D. Noordhuis, A. Prabhu, S.J. Witte, A.Y. Chen, F. Cruz and C. Weniger, *Novel Constraints on Axions Produced in Pulsar Polar-Cap Cascades*, *Phys. Rev. Lett.* **131** (2023) 111004 [2209.09917].
- [268] D. Cadamuro and J. Redondo, *Cosmological bounds on pseudo Nambu-Goldstone bosons*, *JCAP* **02** (2012) 032 [1110.2895].
- [269] J.W. Foster, M. Kongsore, C. Dessert, Y. Park, N.L. Rodd, K. Cranmer et al., *Deep Search for Decaying Dark Matter with XMM-Newton Blank-Sky Observations*, *Phys. Rev. Lett.* **127** (2021) 051101 [2102.02207].
- [270] P. Arias, D. Cadamuro, M. Goodsell, J. Jaeckel, J. Redondo and A. Ringwald, *WISPy Cold Dark Matter*, *JCAP* **06** (2012) 013 [1201.5902].
- [271] C.B. Adams et al., *Axion Dark Matter*, in *Snowmass 2021*, 3, 2022 [2203.14923].
- [272] M. Gorghetto and G. Villadoro, *Topological Susceptibility and QCD Axion Mass: QED and NNLO corrections*, *JHEP* **03** (2019) 033 [1812.01008].
- [273] XENON collaboration, *Excess electronic recoil events in XENON1T*, *Phys. Rev. D* **102** (2020) 072004 [2006.09721].
- [274] XENON collaboration, *Emission of single and few electrons in XENON1T and limits on light dark matter*, *Phys. Rev. D* **106** (2022) 022001 [2112.12116].
- [275] XENON collaboration, *Search for New Physics in Electronic Recoil Data from XENONnT*, *Phys. Rev. Lett.* **129** (2022) 161805 [2207.11330].
- [276] PANDAX collaboration, *Limits on Axion Couplings from the First 80 Days of Data of the PandaX-II Experiment*, *Phys. Rev. Lett.* **119** (2017) 181806 [1707.07921].
- [277] DARKSIDE collaboration, *Search for Dark Matter Particle Interactions with Electron Final States with DarkSide-50*, *Phys. Rev. Lett.* **130** (2023) 101002 [2207.11968].

- [278] EDELWEISS collaboration, *Searches for electron interactions induced by new physics in the EDELWEISS-III Germanium bolometers*, *Phys. Rev. D* **98** (2018) 082004 [1808.02340].
- [279] SUPERCDMS collaboration, *Constraints on dark photons and axionlike particles from the SuperCDMS Soudan experiment*, *Phys. Rev. D* **101** (2020) 052008 [1911.11905].
- [280] GERDA collaboration, *First Search for Bosonic Superweakly Interacting Massive Particles with Masses up to 1 MeV/c² with GERDA*, *Phys. Rev. Lett.* **125** (2020) 011801 [2005.14184].
- [281] P. Gondolo and G.G. Raffelt, *Solar neutrino limit on axions and keV-mass bosons*, *Phys. Rev. D* **79** (2009) 107301 [0807.2926].
- [282] F. Capozzi and G. Raffelt, *Axion and neutrino bounds improved with new calibrations of the tip of the red-giant branch using geometric distance determinations*, *Phys. Rev. D* **102** (2020) 083007 [2007.03694].
- [283] R.Z. Ferreira, M.C.D. Marsh and E. Müller, *Do Direct Detection Experiments Constrain Axionlike Particles Coupled to Electrons?*, *Phys. Rev. Lett.* **128** (2022) 221302 [2202.08858].
- [284] K. Langhoff, N.J. Outmezguine and N.L. Rodd, *Irreducible Axion Background*, *Phys. Rev. Lett.* **129** (2022) 241101 [2209.06216].
- [285] S. Chigusa, M. Hazumi, E.D. Herbschleb, N. Mizuochi and K. Nakayama, *Light Dark Matter Search with Nitrogen-Vacancy Centers in Diamonds*, **2302.12756**.
- [286] S. Chigusa, T. Moroi and K. Nakayama, *Detecting light boson dark matter through conversion into a magnon*, *Phys. Rev. D* **101** (2020) 096013 [2001.10666].
- [287] A. Mitridate, T. Trickle, Z. Zhang and K.M. Zurek, *Detectability of Axion Dark Matter with Phonon Polaritons and Magnons*, *Phys. Rev. D* **102** (2020) 095005 [2005.10256].
- [288] T. Ikeda, A. Ito, K. Miuchi, J. Soda, H. Kurashige and Y. Shikano, *Axion search with quantum nondemolition detection of magnons*, *Phys. Rev. D* **105** (2022) 102004 [2102.08764].
- [289] D.F. Jackson Kimball et al., *Overview of the Cosmic Axion Spin Precession Experiment (CASPEr)*, *Springer Proc. Phys.* **245** (2020) 105 [1711.08999].
- [290] J. Lee, M. Lisanti, W.A. Terrano and M. Romalis, *Laboratory Constraints on the Neutron-Spin Coupling of feV-Scale Axions*, *Phys. Rev. X* **13** (2023) 011050 [2209.03289].
- [291] C. Abel et al., *Search for Axionlike Dark Matter through Nuclear Spin Precession in Electric and Magnetic Fields*, *Phys. Rev. X* **7** (2017) 041034 [1708.06367].
- [292] NASDUCK collaboration, *New constraints on axion-like dark matter using a Floquet quantum detector*, *Sci. Adv.* **8** (2022) abl8919 [2105.04603].
- [293] NASDUCK collaboration, *Constraints on axion-like dark matter from a SERF comagnetometer*, *Nature Commun.* **14** (2023) 5784 [2209.13588].
- [294] JEDI collaboration, *First Search for Axionlike Particles in a Storage Ring Using a Polarized Deuteron Beam*, *Phys. Rev. X* **13** (2023) 031004 [2208.07293].
- [295] K. Wei et al., *Dark matter search with a strongly-coupled hybrid spin system*, **2306.08039**.
- [296] Z. Xu et al., *Constraining Ultralight Dark Matter through an Accelerated Resonant Search*, **2309.16600**.
- [297] M. Buschmann, C. Dessert, J.W. Foster, A.J. Long and B.R. Safdi, *Upper Limit on the QCD Axion Mass from Isolated Neutron Star Cooling*, *Phys. Rev. Lett.* **128** (2022) 091102 [2111.09892].
- [298] T. Nakama, J. Silk and M. Kamionkowski, *Stochastic gravitational waves associated with the formation of primordial black holes*, *Phys. Rev. D* **95** (2017) 043511 [1612.06264].
- [299] J. Garcia-Bellido, M. Peloso and C. Unal, *Gravitational Wave signatures of inflationary models from Primordial Black Hole Dark Matter*, *JCAP* **09** (2017) 013 [1707.02441].

- [300] R.-g. Cai, S. Pi and M. Sasaki, *Gravitational Waves Induced by non-Gaussian Scalar Perturbations*, *Phys. Rev. Lett.* **122** (2019) 201101 [[1810.11000](#)].
- [301] N. Bartolo, V. De Luca, G. Franciolini, A. Lewis, M. Peloso and A. Riotto, *Primordial Black Hole Dark Matter: LISA Serendipity*, *Phys. Rev. Lett.* **122** (2019) 211301 [[1810.12218](#)].
- [302] N. Bartolo, V. De Luca, G. Franciolini, M. Peloso, D. Racco and A. Riotto, *Testing primordial black holes as dark matter with LISA*, *Phys. Rev. D* **99** (2019) 103521 [[1810.12224](#)].
- [303] W. Qin, S.R. Geller, S. Balaji, E. McDonough and D.I. Kaiser, *Planck constraints and gravitational wave forecasts for primordial black hole dark matter seeded by multifield inflation*, *Phys. Rev. D* **108** (2023) 043508 [[2303.02168](#)].
- [304] S. Kumar, R. Sundrum and Y. Tsai, *Non-Gaussian stochastic gravitational waves from phase transitions*, *JHEP* **11** (2021) 107 [[2102.05665](#)].